NASA TECHNICAL NOTE

NASA TN D-3443

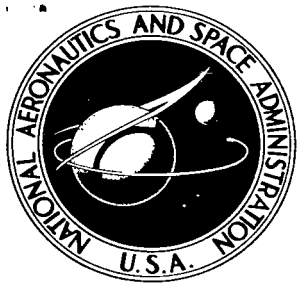

GROUND MEASUREMENTS OF SHOCK-WAVE PRESSURE FOR FIGHTER AIRPLANES FLYING AT VERY LOW ALTITUDES AND COMMENTS ON ASSOCIATED RESPONSE PHENOMENA

by Domenic J. Maglieri, Vera Huckel, and Tony L. Parrott

Langley Research Center
Langley Station, Hampton, Va.

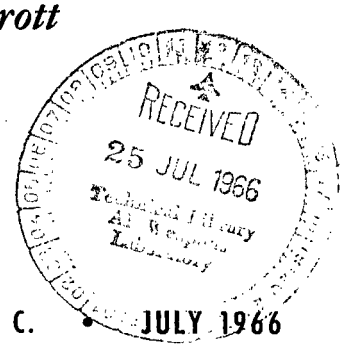

NATIONAL AERONAUTICS AND SPACE ADMINISTRATION • WASHINGTON, D. C. • JULY 1966

GROUND MEASUREMENTS OF SHOCK-WAVE PRESSURE FOR FIGHTER AIRPLANES FLYING AT VERY LOW ALTITUDES AND COMMENTS ON ASSOCIATED RESPONSE PHENOMENA

By Domenic J. Maglieri, Vera Huckel,
and Tony L. Parrott

Langley Research Center
Langley Station, Hampton, Va.

NATIONAL AERONAUTICS AND SPACE ADMINISTRATION

For sale by the Clearinghouse for Federal Scientific and Technical Information
Springfield, Virginia 22151 – Price $3.00

GROUND MEASUREMENTS OF SHOCK-WAVE PRESSURE FOR FIGHTER AIRPLANES FLYING AT VERY LOW ALTITUDES AND COMMENTS ON ASSOCIATED RESPONSE PHENOMENA[1]

By Domenic J. Maglieri, Vera Huckel,
and Tony L. Parrott
Langley Research Center

SUMMARY

Extensive ground measurements of shock-wave pressure have been made for two different supersonic fighter airplanes in the Mach number range of about 1.05 to 1.16 and for altitudes from about 50 to 890 feet. Comparisons of the pressure rises across the shock wave measured on the ground are made with the available theoretical data, and these pressure data are correlated with some data on window-glass breakage. Brief discussions are also given relative to other associated phenomena such as ground motions and response of equipment and personnel.

The pressure time histories measured at ground level were found to contain more peaks than would be obtained at ground level from flights at high altitudes. These pressure peaks seemed to be associated with features of the airplane geometry. The measured values of pressure rise across the bow shock wave decreased with increasing altitude as predicted by theory. There is, however, a tendency for the theory to overestimate the pressure rises measured at ground level, the "near field" theory being in better agreement with the measured results than the prediction obtained with the "far field" theory.

Results from the window-breakage experiments indicated that of 214 possible breakages of window models (3- by 3-foot plain and colonial residential types), 51 breakages actually occurred within the pressure range of about 20 to 100 pounds per square foot experienced during the tests. As might be expected, a higher percentage of failures generally occurred with increased peak pressure rise across the shock wave. It was also found that the detail characteristics of the pressure time histories are significant; and in line with some theoretical considerations, more damage occurred for the time histories having longer time durations of the first positive pressure rise across the shock wave.

---

[1]Supersedes recently declassified NASA TM X-611 by Domenic J. Maglieri, Vera Huckel, and Tony L. Parrott, 1961. No attempt is made to update this material to reflect the current state of the art.

INTRODUCTION

Some incipient nuisance damage such as window-glass breakage has been caused by sonic booms from airplanes in normal high-altitude operations (refs. 1, 2, and 3). There have also been a few instances where rather severe damage has been done in a localized area due to a low-altitude pass at supersonic speeds (ref. 4). This severe damage consisted of widespread window and plaster damage and, in some instances, the buckling of foundations, walls, and roofs. Because of the increased performance capabilities of some proposed supersonic airplanes, it will be possible to operate at supersonic Mach numbers at very low altitudes and over fairly long distances. Thus there will be the capability for exposing large areas to intense sonic booms for possible tactical purposes.

The question has arisen as to the possibility of doing enough damage as a result of the sonic boom to warrant its use as a tactical weapon against structures, equipment, and personnel. In order to answer this question information is needed in two general areas; namely, the nature of the pressure time histories available from low-level airplane operations and an understanding of their significance with respect to the response of structures, equipment, and personnel.

Information is available relative to both the near-field and far-field shock-wave patterns of fighter and bomber airplanes in high-altitude flight (refs. 1, 5, 6, 7, 8, 9, and 10). Methods for calculating the shock-wave intensities in the far field are given in reference 11, 12, 13, and 14, and in the near field in references 7 and 8. The pressure time histories at ground level have been measured for a fighter airplane for altitudes as low as 5,000 feet in the work of reference 2. Only a small amount of well documented information is available relative to the damage caused by sonic booms (refs. 1, 2, 3, 4, and 15), and in no case has extensive damage to ground installations been correlated with shock-wave pressure measurements. Consequently, a flight-test program sponsored jointly by the Tactical Air Command of the U.S. Air Force and the National Aeronautics and Space Administration was performed to obtain this information.

The main purpose of the present paper is to present the results of extensive ground measurements of shock-wave pressure from fighter airplanes during this flight-test program which was previously discussed briefly in reference 15. These pressure data are correlated with some window-glass breakage. Brief discussions are also given relative to other associated phenomena such as ground motions and response of equipment and personnel.

SYMBOLS

A	airplane cross-sectional area, sq ft
a	edge dimension of window, in.
l	airplane length, ft
M	airplane Mach number
s	lateral distance from airplane flight path, miles
T	period of fundamental vibration mode of window, sec
V	airplane ground velocity, ft/sec
x	cylindrical coordinate measured along body axis, ft
Δp_f	pressure rise across shock wave in free air, lb/sq ft
Δp_o	pressure rise across shock wave at ground level, lb/sq ft
Δt	time interval between arrival of bow shock wave and tail shock wave, sec
η	time duration of initial positive phase of shock-wave pressure time history, sec
μ_{exp}	experimentally determined shock-wave angle, deg
τ	window-glass thickness, in.

APPARATUS AND METHODS

Test Conditions

The experimental setups were located on a dry lake bed in Range 3 of the Las Vegas Bombing and Gunnery Range which is about 50 miles north of Las Vegas, Nevada at an altitude of 3,000 feet (fig. 1). The lake bed, with a dry sand and clay sedimentary surface, is about 2 miles wide and about 5 miles long and is located in a broad valley between two high mountain ridges about 40 miles apart. It is isolated from surrounding populated areas by about a 10-mile distance in all directions. Shown superposed on the contour map of figure 1 is the "run-in" line used as

a visual reference by the pilots during the test flights on a heading of about 300° magnetic. Also indicated on the map are the locations of the weather station and the optical airplane tracking unit. Tests were made during July 1960 in the early morning hours while the atmospheric turbulence was a minimum. The photograph of figure 2 shows some features of the test area including a view of the experimental setups.

Test Airplanes

Two different fighter airplanes operated by personnel of the Tactical Air Command were used in the flight tests. Photographs including side, three-quarter front, and front views are presented in figures 3 and 4 for airplanes A and B, respectively. Equivalent body area distributions for airplanes A and B are given in figure 5. The solid curves in both cases include the full inlet capture area, whereas the dashed curve for airplane B has been adjusted to account for the inlet open area. Airplane A of figure 3 has a length of 54.7 feet, a wing span of 26.2 feet, a gross weight of 27,000 pounds, and a maximum installed static thrust of 17,500 pounds. Airplane B of figure 4 has a length of 64.8 feet, a wing span of 34.3 feet, a gross weight of 34,000 pounds, and a maximum installed static thrust of 22,500 pounds. The airplanes were at all times operated without external fuel tanks.

Airplane Operation and Positioning

Prior to a test run, the aircraft loitered at an altitude of about 17,000 feet, dived to an intermediate altitude at about 10 miles downrange from the test area, accelerated to supersonic speeds in shallow dives to a point about 5 miles from the test area, and then approached at steady-flight conditions on a heading of about 300° magnetic along the run-in line of the bombing range (fig. 1). These flights were made in the altitude range of 50 feet to about 890 feet and for the Mach number range of 1.05 to 1.16. A summary of the airplane operation data for all flights under steady conditions is given in table I along with estimated ambient temperature at flight altitude.

For a special test some supersonic passes were made over a two-engine transport airplane airborne at a low altitude (wheels about 5 to 30 feet above the lake-bed surface) and at a vertical-separation distance of from 300 to 1,000 feet.

In all cases the aircraft were positioned over the test area by the pilot with the aid of visual observations of the bombing run-in line. Observations by various ground observers in the test area indicated that the pilots did not deviate appreciably in a lateral direction from the overhead position. Optical tracking equipment located at a perpendicular

distance of about 5 miles from the run-in line (fig. 1) was used to track the test airplanes for purposes of obtaining altitude and speed information. Supplementary information on airplane speed was obtained with a microphone speed trap set up in the test area. During early morning hours when lighting conditions were poor, it was not possible to obtain optical tracks on some of the test flights.

Atmospheric Soundings

Weather observations at intervals of 100 feet were made up to an altitude of 500 feet at a location approximately $1\frac{1}{2}$ miles from the test area as indicated in figure 1. Temperature and humidity data were obtained by means of wiresonde (captive balloon) equipment. Wind velocity and gradients were measured by means of a constant-rate-of-ascent balloon and a double phototheodolite tracking setup. Observations were made approximately every 20 minutes during the time intervals of the tests. The wind and dewpoint data obtained are listed in table II, and the temperature gradients are plotted in figure 6 along with a curve representing the ICAO standard atmosphere temperature gradient (ref. 16).

It can be noted that the weather conditions were similar from day to day and changed by only a small amount during the time interval of each test. Surface winds varied from 0 to about 10 knots and surface temperatures were in the range 60° F to 80° F. Very well defined temperature inversions existed during the test periods, the temperature at 500 feet being in some cases about 20° F higher than the surface temperature.

Pressure Measurement Instrumentation

Ten condenser microphones for measuring the shock-wave pressures were located on the ground track and at distances up to 0.5 of a mile in the lateral direction. (See sketch of fig. 7.) Eight of these microphones had a useful frequency range from about 5 to 10,000 cps, a flat frequency response (within ±2 db) in the range from 10 to 7,000 cps, and were calibrated with a 400 cps sine wave at a pressure level of 121 db. The other two microphones had a usable frequency range of approximately 0.5 to 10,000 cps and were calibrated with a 400 cps sine wave at a pressure level of 146.5 db.

The signals from all microphones were recorded simultaneously on a frequency-modulated tape recorder having a flat frequency response from 0 to 10,000 cps. Tape playbacks of the pressure time histories were recorded on an oscillograph having galvanometer elements, the frequency responses of which were flat from 0 to 5,000 cps. All the microphones

were shock mounted in 3/4-inch plywood boards which, in turn, were securely anchored by corner stakes to the ground for the ground measurements. Provisions were made for measuring the shock-wave pressure in free air as well as the reflected component. From the preceding measurements, calculations of the incident and reflected pressures, the ground-reflection coefficients, and the airplane ground speeds and shock-wave angles were made. For some special experiments, sound-pressure measurements were made both inside and outside of a window mounted on a test cubicle.

Four mobile microbarograph stations incorporating pressure measuring and recording equipment covering the frequency range from 0 to 30 cps were supplied by the Sandia Corporation and were used to obtain data at distances from approximately 0.4 to 2 miles from the flight path in a lateral direction, as indicated in figure 7.

Glass-Breakage Experiments

Window-glass models of each of two different window styles were attached to plywood and frame cubicles and positioned in the test area to study glass-breakage phenomena. The two types of windows tested and one of the test cubicles are shown in the photograph of figure 8. The plain window contains glass approximately 1/8 of an inch thick and approximately 3 feet square. The colonial window incorporates 9 panes of glass, each of which is approximately 3/32 of an inch thick and approximately 11 inches square. Standard wooden frames and mullions were used.

For purposes of the tests, these windows were attached to cubicles having internal volumes ranging from approximately 16 cubic feet (shown in fig. 8(b)) to 96 cubic feet. These cubicles with the windows attached were then arranged in various orientations with respect to the flight direction, at various distances from the flight track, and in several multiple arrangements. The test models were arranged in the same general areas as the pressure measurement instrumentation so that damage results could be correlated with the pressures. Sketches of the test arrangements of the window models showing the model numbers, location, and orientation for each of the 4 days on which flights were made are shown in figure 9.

In order to study the behavior of glass fragments from windows damaged by sonic booms, a missile-trap section (see fig. 7 for location in test area) consisting of a window-glass arrangement mounted in front of a Styrofoam backstop was installed by personnel from The Lovelace Foundation for Medical Education and Research. The objective was to determine whether or not window-glass fragments due to damage induced by sonic boom behaved in a manner similar to those already studied

for atomic and conventional bomb explosions. Provisions were made to measure the size, the distance traveled, and the associated kinetic energy of the fragments.

Other Miscellaneous Experiments

In addition to the pressure measurements and the glass-breakage experiments cited previously, several other experiments were conducted simultaneously.

Environmental test of missile weapons system.- A complete ground-to-ground missile with all of its associated ground transportable launch complex and auxiliary equipment (see fig. 10) was provided by the Tactical Air Command in an experiment to determine possible deleterious effects of intense sonic booms on its operation. The equipment was arranged in such a manner that the regular prelaunch, launch, and post-launch operations and operational checks could be performed.

Airplane structural and control response.- A transport airplane (fig. 11) instrumented by strain gages to measure the response of wing and horizontal-tail surfaces and selected skin panels was parked in the test area.

Provision was also made to fly the airplane at low altitude (about 5 feet to 30 feet above the lake-bed surface) during several supersonic passes by fighter airplanes (approaching from the rear) at vertical separation distances of about 300 to 1,000 feet.

Observations of human response.- Personnel from the Aeromedical Laboratory of the Wright Air Development Division observed the tests to determine whether or not there were any significant adverse human reactions to the intense sonic booms in these tests.

Ground-motion studies.- Seismic pickups were oriented to measure ground motions in both the horizontal and vertical directions and were located near the ground track of the airplane. (See relative location in fig. 7.) Each seismic pickup consisted of a coil moving in a magnetic field, the electrical output being proportional to velocity. The output signals were electrically integrated to give displacement and were recorded in such a manner that ground-motion amplitudes and frequencies could be determined. The seismic pickups were buried approximately 5 feet underground. Prior to installation, these units were calibrated on a shake table at frequencies from 2 to 100 cps.

Measurements of airplane vertical acceleration.- VGH recorders were installed in three of the four test airplanes to measure acceleration

at the airplane center of gravity for correlation with measurements of airplane velocity and altitude during the low-altitude supersonic test flights. The recording equipment operated during the entire flight, and special provision was made to indicate on the records that part of the run during which the airplane was at supersonic speeds and at low altitudes.

DISCUSSION OF RESULTS

Measured Pressure Time Histories in Level Flight

Wave shapes.- Tracings of some selected time histories from which data were obtained are reproduced in figures 12 to 19 to illustrate some of the physical phenomena involved. It should be noted that the time scales are comparable for all of the tracings shown but that because of differences in gain settings, the amplitudes are not necessarily comparable. All time-history records presented were obtained with microphones having a frequency response flat within ±2 db from 10 to 7,000 cps. The time histories of the shock noise pressures from flight 24 of airplane A as obtained at ground level and on a 20-foot-high mast are presented in figures 12(a) and 12(b), respectively. Several distinguishing features are noted. For instance, in figure 12(a) there is first a very rapid pressure rise followed by two smaller compressions before the final recompression takes place. The general shapes of these waves are similar to those measured from airplanes at high altitudes in the probe flight tests of references 6 and 8. They do, however, differ in detail probably because of the differences in distance and orientation of the airplane with respect to the measurement apparatus. Since the time history of figure 12(a) was measured at ground level, the incident and reflected waves are coincident. On the other hand, the measured trace obtained at the top of a 20-foot-high mast, as shown in figure 12(b), contains separate incident and reflected wave components since, in this case, the reflected wave arrives at the measuring station at some time interval later than the incident wave.

As indicated in figure 12(a), the quantity Δp_o is the pressure rise associated with the passage of the bow shock wave and is the amount by which the local atmospheric pressure is exceeded at ground level. Likewise, Δp_f is the pressure rise in free air due to the passage of the bow shock wave. Measured values of the quantities Δp_o and Δp_f as presented in table III represent a summary of the measured pressures obtained on the flight path and at various lateral stations for all flights of airplanes A and B for which data were obtained. The ratio $\Delta p_o/\Delta p_f$ is called the reflection factor which, for a perfect reflecting surface, has a theoretical value of 2. The quantity Δt is defined as the time interval between the arrival of the bow shock wave and the tail shock wave. The values of Δt listed in table IV were obtained from ground-level measurements.

Time histories of the shock noise pressures for flight 15 of airplane B as obtained at ground level and on top of a 20-foot-high mast are presented in figure 13. The same general conclusions may be drawn from these data as for the data of figure 12. It is, however, evident that the pressure time histories for airplane B are much more complex than those for airplane A. The reason for this is suggested by the sketches and associated measured data of figures 14 and 15.

It may be seen that a rough correlation exists between the discontinuities in the pressure traces and the protuberances in the external geometry of the airplanes. This correlation is especially evident in figure 15 which relates to airplane B, since in this case each pressure discontinuity occurs at a time interval consistent with the geometric protuberances on the airplane and the airplane passing rate. In figure 14, which applies to airplane A, this is believed also to be the case although it is not so readily evident from the figure.

It was found from the measurements that each airplane had a characteristic time-history shape and that these time histories developed in an orderly manner as a function of Mach number and distance from the airplane. The manner in which this development occurs can be illustrated for the two airplanes by the data of figures 16 and 17. Figure 16 includes tracings of pressure time histories measured at the ground for airplane A for an altitude range from about 60 to 590 feet and for a Mach number range from 1.065 to 1.145. The traces are arranged in the order of increasing altitude reading from top to bottom in such a way that their periods can be compared directly. It can be seen from a comparison of the traces of figure 16(c) with 16(e) which are for nearly equal Mach numbers that the period increases as altitude increases.

Figure 17 includes tracings of pressure time histories measured at the ground for airplane B for an altitude range from about 50 to 320 feet and for a Mach number range from 1.118 to 1.155. It can be seen from a comparison of the traces of figure 17(b) with those of figure 17(c) which are for nearly equal altitudes that the period decreases as Mach number increases. In the case of airplane B the measured pressure time histories had essentially the same detailed structure at the lower altitudes as at the higher altitudes of the tests. In the case of airplane A, however, it was noted that the time histories for the lower airplane altitudes exhibited a rounded-off appearance as in the trace of figure 16(a). This result suggests that the individual shock waves may not have been able to coalesce with the bow shock wave for this particular airplane at these close separation distances.

It was noted during these tests that the pressure time histories measured at the ground also varied in an orderly manner as a function of lateral distance from the flight path. As an illustration, pressure time-history tracings at two lateral distances from the flight path are

presented in figure 18 for test flight 4 of airplane B. One obvious result is that the periods of the waves increase with increased lateral distance. It may also be seen that the measured traces at the greater distances from the flight path have fewer pressure peaks. The differences in the pressure time histories of figure 18 may be due to differences in the angles of observation and the tendency for the smaller pressure peaks to coalesce as the wave pattern propagates to larger distances.

During the flight tests an attempt was made to change the pressure time histories of airplane B by deploying its speed brakes. It was believed that the peak pressures might be increased for a short segment of the flight because of the sizable increase in drag associated with the deployment of the brakes. The pressure time histories obtained with and without the brakes deployed are presented in figure 19 for locations on the flight path and at a lateral distance from the track of 0.25 mile.

The deployment of the brakes which are located at the rear of the airplane, two in a horizontal plane and two in a vertical plane (see fig. 4(a)), resulted in an additional peak in the pressure time history as indicated in figure 19(a). At the measuring station at $s = 0.25$ mile no additional peak seemed to be present due to the deployment of the brakes. It is believed that the deployment of the brakes did not measurably affect the bow-wave peak pressure rises at these distances.

Periods.- Data relating to the periods of the pressure time histories are included in table IV in which both measured and calculated values are given for all of the test runs. Calculations of the time intervals have been made with the far-field expression of reference 11 as presented in reference 1, and also by the following expression:

$$\Delta t = \frac{l}{V}$$

It can be seen that in general the values calculated by the preceding expression, which does not account for the normal spreading of the waves, are in better agreement with the measurements obtained close to the aircraft than those calculated by the method of reference 11. At the larger distances, however, the values calculated by the method of reference 11 are in better agreement. It is significant to note that the calculations by the method of reference 11 are consistently lower than measured values at the short distances but are in very good agreement with the measured values at distances greater than 0.25 mile.

Peak pressures.- Measured peak-pressure data are listed in tables III(a) and III(b) for airplanes A and B, respectively. Values

of Δp_o are listed for individual microphones at positions on the flight path and at lateral distances up to 0.5 mile. Shown also for comparison are theoretical values of Δp_o calculated by the far-field relations of reference 11 in the form presented in reference 1 and by the near-field relations of reference 7. All of the calculated values listed in tables III(a) and III(b) include a ground reflection factor of 1.8 to make them comparable to ground measurements. Some measured values of Δp_f are also presented.

The measured data for all microphones located on the track are plotted in figure 20 for airplane A in order to illustrate the trends of the measured pressures as a function of airplane altitude. Shown also for comparison are calculated curves by the methods of references 7 and 11 for an assumed Mach number of 1.13. It can be seen in figure 20(a) that the values for pressure rise across the shock wave measured at the ground range from about 20 pounds per square foot at 600 feet altitude to about 100 pounds per square foot at 60 feet altitude. Although a considerable amount of scatter exists in the data, it may be seen that the measured values are consistently lower than those calculated by the far-field method of reference 11. However, the general trend of the data as a function of altitude seems to be predicted by the theoretical curve, and thus the theory of reference 11 is useful for making extrapolations to the near field.

The calculated values for the near field shown in figure 20(a) were obtained from the work of Donald L. Lansing of the Langley Research Center by the method of reference 7. These values are in better agreement with the measured values over the whole range of altitudes but are also consistently higher than the measured values.[2] Similar conclusions may be drawn from the comparison of measured with calculated free-air values of figure 20(b). An analysis of the experimental results indicated that the pressures measured at the ground were higher than those measured in the free air by a factor which varied from about 1.7 to 2.0 for these near-field tests. The preceding reflection-coefficient values are, thus, in general agreement with those reported in reference 1.

Similar data for airplane B are given in figure 21. The pressures are seen to be in approximately the same range as for airplane A although more scatter is apparent in the pressure data measured at the ground. (See fig. 21(a).) The general trends of the pressure for airplane B as a function of altitude are also predicted by the theoretical curves. As

[2]Subsequent to the original release of the present report (1961), W. D. Middleton and H. W. Carlson in NASA TN D-3082 have published a more sophisticated method for computing the near-field curves than was used to obtain the curves in figures 20 and 21.

was the case with airplane A, the pressures calculated with the near-field theory are in better agreement with the measurements.

In general, the measurements of figures 20 and 21 indicated that although the detailed structure of the pressure time histories differed for the two airplanes, the peak bow-wave pressure rises were not markedly different even though the gross weight of airplane B was greater than that of airplane A by a factor of nearly 1.3.

Lateral spread patterns.- In addition to the measurements on the track, peak pressure data were also obtained by means of microphones at distances up to 0.5 of a mile in a direction perpendicular to the flight path. (See fig. 7.) These data, which are listed in table III, along with microbarograph data supplied by the Sandia Corporation are plotted in figures 22 and 23 for airplanes A and B, respectively, in order to illustrate the trends of the pressures measured at the ground as a function of lateral distance. Pressure data measured at the ground for four altitude ranges are grouped together for each airplane. Those data points with ticks in figure 22 were obtained from pressure measurements in free air multiplied by a reflection factor of 1.8. Shown also in figures 22 and 23 for comparison are calculated lateral-spread curves from the method of reference 11 for the mean altitude of each group of data and for a Mach number of 1.13. The calculated cutoff distances due to refraction are based on the method of reference 12 for which a normal temperature gradient is assumed and are indicated in the figures by the vertical dashed lines. It can be seen that the calculated curves decrease rapidly with lateral distance. The data points also decrease rapidly in magnitude with lateral distance and are noted to be roughly symmetrical. In all cases the shock-wave pressures were observed (although data points may not be shown) at distances beyond the calculated cutoff distance for a normal temperature gradient. It is believed that the reason booms were observed beyond the calculated cutoff distances was that temperature inversions and very low velocity surface winds were measured during the times of these flights. (See fig. 6 and table II.)

Window-Glass Breakage

Static loading tests.- In order to determine the static strength of the window models used in the tests, a series of laboratory tests was performed. These tests were made by assembling the windows and cubicles similar to the manner in which they were assembled for the flight tests with the exception that the putty side was turned inward. A uniform positive pressure was applied to the putty side of the window surface. The results of these static-loading tests are shown in figure 24. Maximum deflection of the glass in inches is shown as a function of the pressure load in pounds per square foot for a plain window. The window deflection is seen to increase as the load increases until

a break occurs, as indicated by the solid symbol, at a pressure of about 155 pounds per square foot. The other solid symbols (not on the curve) represent breaking points of similar windows obtained in other tests. Some scatter is expected in the breaking loads for these windows because of observed variations in glass thickness and possible variations in glass surface and mounting conditions. As a matter of interest, it was noted that a window having a surface scratch on the tension side failed at about 15 percent of the pressure load required to fail on an unscratched model. An attempt was made to mount the models in such a way as to minimize torsional or shear loads applied to the glass surfaces.

The results of similar studies for the colonial windows indicated considerably larger deflections for the same applied static-pressure loads. These larger deflections are believed to be caused by the inherent flexibility of the mullions. The static breaking loads for the colonial windows were noted to be about one-half of those for the plain windows of figure 24. When the mullions were restrained from deflecting, however, it was found that the unit pressure loading at which failure occurred for the 1- by 1-foot glass panes was about the same as that for the 3- by 3-foot glass panes of the plain windows.

Dynamic properties of windows and cubicles.- During laboratory tests the opportunity was taken to obtain the natural frequencies of these two types of windows. As a result of these tests it was found that the plain windows had a fundamental vibration mode at about 28 cps, a second mode at about 47 cps, and a third mode at about 80 cps. In the case of the colonial window the fundamental mode was found to be at about 43 cps and the second mode at about 66 cps. The first-mode frequencies of the individual glass panels of the colonial windows were found to be in the range of 120 to 160 cps.

Results of flight tests.- During the flight-test program, 214 window-glass breakage experiments were performed with the models located as indicated in figure 9 for each day of the flight tests. Detailed information relative to the test conditions for each window model is listed in table V. Such information as the window test location, the type of window, the estimated pressure rise across the shock wave, and the damage, if any, that was incurred for each flight number is given. A blank in the damage column indicates that no test data were obtained. It can be seen that a total of 51 damage points was obtained. From these results it was not possible to attach any particular significance to the volume of the cubicle nor to the angle of the window pane with respect to the flight direction. When grouped in a multiple arrangement, however, it was determined that the glass panels near the center of the arrangement and also toward the ground surface seemed to be most susceptible to damage. Photographs of typical damage are shown in figure 25.

In an attempt to illustrate the main findings of the tests, the pertinent data of table V have been summarized in the form of a bar graph in figure 26. The data are arranged to indicate the nature of the individual results obtained in five ranges of pressure rises from 0 to 100 pounds per square foot. Since damage occurred for both the plain and colonial windows over the same ranges of pressures, the results have been combined for the purposes of this figure. Each bar represents the percentage of the total number of test models that failed for each airplane during the tests at the respective pressures indicated. The hatched areas represent data obtained with airplane A, whereas the cross-hatched areas represent data obtained with airplane B. It can be seen that no failures occurred at pressures below 20 pounds per square foot. However, it should be noted that no windows were exposed to this pressure range for airplane A. In the range of pressures from 20 to 100 pounds per square foot, a larger percentage of the models was damaged at the higher pressures. It can also be seen that failures occurred at lower pressure rises for the pressure time histories of airplane A than for those of airplane B; thus differences in the details of the pressure time histories as illustrated in the sketches at the top of figure 26 may be significant with respect to window-glass breakage.

One of the obvious differences in the pressure time histories of the two airplanes, as illustrated in figures 16 and 17, is the time duration of the initial positive phase. Consequently, an attempt was made to correlate the available experimental glass-breakage data for plain windows with the detail characteristics of this initial positive phase of the pressure time history, and the results are given in figure 27. The ordinate is the product of the pressure rise across the shock wave measured at the ground Δp_o and the square of the ratio of the edge dimension of the window to the glass thickness. This latter factor, involving window dimensions, normalizes the stress per unit area for different size windows of the same shape and same edge support condition. The abscissa is the ratio of the time duration of the initial positive phase of the shock-wave pressure time histories to the period of the fundamental mode of the window. The theoretical curve is based on information presented in figure 33 and table VI of reference 4 and is for a pressure time history having an initial positive phase equal to about one-sixth of the total period Δt. This curve applies directly to square windows clamped on all edges. Values of the ordinate which fall above the curve are associated with damage, whereas for values below this curve no damage should occur.

The circular data points represent the results of the low-altitude flights of the present tests for 3- by 3-foot plain windows. The square and diamond data points represent the results of high-altitude flights for square windows of references 10 and 9, respectively. The triangular

data points representing the results of tests on large rectangular windows (refs. 10 and 1) are also included in the figure for additional information. Solid symbols in all cases indicate damage points.

It will be noted that all of the damage points for the square windows fall above the curve and thus in the theoretical damage region. The only damage point falling below the theoretical curve is associated with a large plate-glass store front window (ref. 1). This window was the center pane of three similar size windows and was restrained mainly at the top and bottom. All of the windows with the exception of the large windows of references 1 and 10 were mounted in such a way that the prestressing due to the mounting was minimized.

During the window-breakage experiments there was opportunity to observe the manner in which glass fractures were initiated as well as the behavior of the glass fragments. High-speed motion pictures indicated that in at least one instance a plain window failed on the second cycle of inward deflection. Failure was very rapid and a large number of radial cracks extending from near the center to the edges was noted to exist. When failure was severe enough so that glass fragments were dislodged from the window, these were noted to come to rest at the base of the window and in close proximity to it as is seen in the photographs of figure 25. Similar results were obtained from the missile-trap experiment performed by The Lovelace Foundation for Medical Education and Research.

With regard to the colonial windows, it was noted that the flexibility of the mullions played a significant role in the subsequent glass failures. In fact, in one instance for which high-speed motion pictures were available, the initial failure was apparent in the mullion bordering the center pane of glass, and shortly after this mullion failure substantial glass breakage was noted. It was noted as a general result of the tests that the middle pane of glass of the colonial windows was most susceptible to damage as is illustrated in figure 25, and frequently this type of failure occurred without any other noticeable damage.

In many cases unmounted windows (not affixed to the cubicle) were exposed to the extreme range of pressure rises (20 to 100 lb/sq ft) indicated in figure 26, and no damage whatsoever was observed. It is believed that because of the absence of the cubicle the pressure tended to equalize and hence no appreciable pressure differential existed across the glass surface. The data of reference 17 indicate that similar windows exposed to blast waves from high explosives were damaged at values of pressure rise across the shock wave in the range of 14 to 108 pounds per square foot. At least part of the scatter in these results is attributed to the wide variations in the mounting details.

Other Measurements and Observations

Response of missile weapons system.- During the preceding flight tests, only minor mechanical damage was suffered by the missile weapons system being tested, and the damage was not of a nature that would prevent the equipment from performing its assigned functions. It was concluded that sonic-boom pressures in the range generated during these tests would not have any significant effects on such rugged electronic equipment, which was designed for operation under conditions of blast loading at overpressures up to 6 pounds per square inch.

Aircraft structural and control response.- Measurable strains were recorded at all strain-gage locations on the transport airplane surfaces, and motions of the tail and wing surfaces were noted during each pass of the supersonic test airplanes. Some very minor damage and unusual occurrences were also noted during these tests but none were judged to affect significantly the safety of the airplane. During low-level flight tests of the transport airplane under the flight path of the supersonic test airplanes at vertical separation distances of approximately 300 to 1,000 feet, the pilots reported that they could hear and feel the shock waves but that no control problems occurred nor did the transport airplane have any appreciable response.

Observations of human response.- No significant adverse physiological reactions were noted. Ear muffs were useful in reducing the intensity of the audible noise although they were not considered necessary by the test operators. Some persons not wearing ear protection observed a brief ringing in the ears, and it was believed that a small amount of temporary hearing loss may have occurred. Some observers exposed repeatedly reported a dislike for the booms and found it difficult to make visual observations.

Most observers close to the flight track of the airplane indicated only one auditory impulse, whereas observers at some appreciable lateral distance from the flight track sometimes reported two auditory impulses as is customary from high-altitude sonic booms. It was concluded that sonic booms having peak pressures in the range experienced in these tests do not adversely affect the performance of individuals although they are apt to have a startling effect if the individual is not forewarned.

Ground motions.- Measurable ground motions occurred during all supersonic flights. The motions were in the frequency range of approximately 2 to 10 cps, and the maximum amplitudes were of the order of 0.010 inch in both horizontal and vertical directions. These motions were many times higher than were measured for subsonic aircraft of comparable size and under otherwise similar flight conditions.

Pilot's reactions.- The pilots did not report any unusual operational problems in accomplishing the preceding flight tests. No appreciable turbulence was encountered due probably to the fact that the tests were accomplished during the early morning hours when the ambient temperatures were relatively low. No unusual control problems were encountered.

Shock-wave angles.- Two microphones were located 20 feet apart in a vertical arrangement in such a manner that the shock-wave angles with reference to the ground plane could be measured. Based on the assumption that the aircraft flight vectors were parallel to the ground plane, the preceding results are believed to be a measure of the airplane shock-wave angles. The measured shock-wave angles are compared with predicted Mach wave angles in table VI and are seen to be in good agreement. Based on these results it is concluded that the reflected shock waves from the ground surface did not impinge on any parts of the test airplanes.

CONCLUDING REMARKS

Extensive ground measurements of shock-wave pressure have been made for two different supersonic fighter aircraft in the Mach number range of about 1.05 to 1.16 and for altitudes from about 50 to 890 feet. The following conclusions were reached:

1. The pressure time histories measured on the ground were found to contain more peaks than would be obtained at ground level from flights at high altitudes. These pressure peaks seemed to be associated with features of the airplane geometry, each airplane having its own characteristic pressure time history. Time intervals of the measured time histories increased with increasing altitude and decreasing Mach number.

2. The measured values of pressure rise across the bow shock wave decreased with increasing altitudes as predicted by theory. There is, however, a tendency for the theory to overestimate the pressure rises across the shock wave, the "near field" theory being in better agreement with the measured results than the "far field" theory. Calculations of the time intervals of the pressure time histories based on only the airplane length and velocity are in good agreement with measured values obtained near the aircraft. At larger distances, however, the calculated time intervals based on far-field conditions seem to compare more favorably with measured values.

3. Results from the window-breakage experiments indicated that of the 214 tests of window models (3- by 3-foot plain and colonial residential type), 51 were broken within the pressure range experienced during the tests. A higher percentage of failures generally occurred with increased pressure rise across the shock wave. Because more failures occurred for airplane A than for airplane B, and since these airplanes have markedly different pressure time histories, there is, thus, an indication that the detail nature of the pressure time history is significant with regard to window breakage. As indicated by analytical considerations, more damage occurred for the time histories having longer time durations of the first positive pressure rise across the shock wave. When glass failure occurred, the fragments were noted to come to rest at the base of the window and in close proximity to it.

Langley Research Center,
National Aeronautics and Space Administration,
Langley Air Force Base, Va., September 11, 1961.
(Reissued June 1966.)

REFERENCES

1. Maglieri, Domenic J., Hubbard, Harvey H., and Lansing, Donald L.: Ground Measurements of the Shock-Wave Noise from Airplanes in Level Flight at Mach Numbers to 1.4 and at Altitudes to 45,000 Feet. NASA TN D-48, 1959.

2. Kerr, T. H.: Experience of Supersonic Flying Over Land in the United Kingdom. AGARD Rept. 250, Sept. 1959.

3. Holbeche, T. A.: A Preliminary Data Report on Ground Pressure Disturbances Produced by the Fairey Delta 2 in Level Supersonic Flight. R. & M. No. 3296, British ARC, June 1958.

4. ARDE Associates: Response of Structures to Aircraft Generated Shock Waves. WADC Tech. Rept. 58-169, U.S. Air Force, Apr. 1959, (Available from ASTIA as AD 229 463 L.)

5. Mullens, Marshall E.: A Flight Test Investigation of the Sonic Boom. AFFTC-TN-56-20, U.S. Air Force, May 1956.

6. Jordan, G. H.: Some Aspects of the Shock-Wave Generation by Supersonic Airplanes. AGARD Rept. 251, Sept. 1959.

7. Whitham, G. B.: The Flow Pattern of a Supersonic Projectile. Commun. Pure Appl. Math., vol. V, no. 3, Aug. 1952, pp. 301-348.

8. Smith, Harriet J.: Experimental and Calculated Flow Fields Produced by Airplanes Flying at Supersonic Speeds. NASA TN D-621, 1960.

9. Lina, Lindsay J., and Maglieri, Domenic J.: Ground Measurements of Airplane Shock-Wave Noise at Mach Numbers to 2.0 and at Altitudes to 60,000 Feet. NASA TN D-235, 1960.

10. Maglieri, Domenic J., and Hubbard, Harvey H.: Ground Measurements of the Shock-Wave Noise from Supersonic Bomber Airplanes in the Altitude Range from 30,000 to 50,000 Feet. NASA TN D-880, 1961.

11. Whitham, G. B.: The Behavior of Supersonic Flow Past a Body of Revolution, Far From the Axis. Proc. Roy. Soc. (London), ser. A, vol. 201, no. 1064, Mar. 7, 1950, pp. 89-109.

12. Randall, D. G.: Methods for Estimating Distributions and Intensities of Sonic Bangs. R. & M. No. 3113, Brit. A.R.C., 1959.

13. Walkden, F.: The Shock Pattern of a Wing-Body Combination, Far From the Flight Path. Aero. Quarterly, vol. IX, pt. 2, May 1958, pp. 164-194.

14. Morris, John: An Investigation of Lifting Effects on the Intensity of Sonic Booms. Jour. R.A.S., vol. 64, no. 598, Oct. 1960, pp. 610-616.

15. Anon.: Project Little Boom. TAC-TR-60-18, U.S. Air Force, Sept. 1960.

16. Minzner, R. A., Ripley, W. S., and Condron, T. P.: U.S. Extension to the ICAO Standard Atmosphere - Tables and Data to 300 Standard Geopotential Kilometers. Geophys. Res. Div. and U.S. Weather Bureau, 1958.

17. Perkins, Beauregard, Jr., Lorrain, Paul H., and Townsend, William H.: Forecasting the Focus of Air Blasts Due to Meteorological Conditions in the Lower Atmosphere. Rep. No. 1118, Ballistic Res. Labs., Aberdeen Proving Ground, Oct. 1960.

TABLE I.- AIRPLANE OPERATION DATA FOR STEADY FLIGHT

Flight test	Time	Estimated ambient temperature at flight altitude, °F	Altitude, feet	Mach number	Velocity, V, ft/sec
		Airplane B; July 18, 1960			
1	0542	81	290	[a]1.1	[a]1,250
2	0553	81	240	1.118	1,274
3	0610	81	210	[a]1.13	[a]1,285
4	0615	81	320	[a]1.14	[a]1,294
5	0633	79	50	1.12	1,274
6	0646	81	280	1.119	1,275
7	0658	81	890	[a]1.12	[a]1,274
		Airplane A; July 19, 1960			
8	0558	86	380	1.053	1,210
9	0609	81	200	1.065	1,226
10	0615	78	140	1.074	1,237
11	0629	82	330	1.074	1,229
12	0639	82	340	1.145	1,304
13	0644	77	110	1.149	1,322
		Airplane B; July 20, 1960			
14	0546	86	305	1.163	1,325
15	0552	83	250	1.155	1,351
16	0602	85	110	1.130	1,310
17	0630	82	[a]300	[a]1.16	[a]1,319
18	0635	82	260	1.136	1,316
19	0647	82	125	1.116	1,265
		Airplane A; July 21, 1960			
20	0615	81	485	1.077	1,277
21	0621	81	270	1.092	1,271
22	0628	76	60	1.124	1,268
23	0653	81	590	1.065	1,226
24	0701	77	190	1.068	1,226
25	0705	76	95	1.088	1,243

[a]Estimated value.

TABLE II.- WIND AND DEWPOINT DATA

Time	Surface wind velocity, knots	Surface wind direction, deg	Wind velocity at 500 feet, knots	Wind direction at 500 feet, deg	Surface dewpoint, °F	Dewpoint at 500 feet, °F
July 18, 1960						
0534 to 0547	2	30	2	310	21.9	21.2
0604 to 0617	3	50	4	280	21.4	19.9
0635 to 0649	6	50	1	110	27.1	19.0
July 19, 1960						
0533 to 0542	2	130	2	130	23.6	26.8
0617 to 0626	Calm		2	250	22.4	48.6
0645 to 0655	Calm		2	250	29.9	26.0
July 20, 1960						
0539 to 0549	7	170	8	180	37.3	34.6
0603 to 0614	Calm		1	170	31.7	58.3
July 21, 1960						
0533 to 0543	Calm		Calm		36.8	38.8
0602 to 0609	3	180	1	90	31.5	37.1
0632 to 0640	4	70	1	70	36.1	38.4

TABLE III.- SUMMARY OF MEASURED FREE-AIR AND GROUND PRESSURES

(a) Airplane A

Flight test	Altitude, ft	Mach number	Δp_o, lb/sq ft, along track						Δp_f, lb/sq ft, along track, measured		Δp_f, lb/sq ft, at s = 0.075 mile	Δp_o, lb/sq ft, at -	
			Far-field theory (ref. 11)	Near-field theory (ref. 7)	Measured							s = -0.2 mile	s = 0.25 mile
July 19, 1960													
8	380	1.053	40.7	40.5	32.0	31.8	34.6		16.5		10.6	11.4	11.0
9	200	1.065	67.8	66.6	54.3	57.0	56.4		28.3		13.6	10.9	10.8
10	140	1.074	90.2	86.4	65.6	80.2	84.5		41.0		15.9	14.4	13.8
11	330	1.074	47.3	46.6	35.1	37.8	40.5		19.6		14.4	13.0	15.2
12	340	1.145	50.4	49.3	41.4	43.7	44.0		23.4		15.2	14.0	16.9
13	110	1.149	118.6	108.8	61.6	78.9	74.4		36.9		10.6	16.5	16.0
July 21, 1960													
20	485	1.077	35.4	35.5	31.7		32.1	27.3	18.6	12.7		15.2	
21	270	1.092	56.6	55.8	42.1		49.3	52.1	28.2	25.0		18.0	
22	60	1.124	182.4	104.2	97.5		100.6	86.3	59.2	53.4		13.1	
23	590	1.065	29.9	30.0	24.7		21.3	26.0	13.0	9.6			
24	190	1.068	70.9	69.3	62.0		58.0	66.7	32.0	27.2		12.7	
25	95	1.088	123.5	115.2	79.3		81.3	96.4	36.1	39.7		14.6	

TABLE III.- SUMMARY OF MEASURED FREE-AIR AND GROUND PRESSURES - Concluded

(b) Airplane B

Flight test	Altitude, ft	Mach number	Δp_o, lb/sq ft, along track					Δp_f, lb/sq ft along track, measured		Δp_o, lb/sq ft, at -		
			Far-field theory (ref. 11)	Near-field theory (ref. 7)	Measured					s = -0.2 mile	s = 0.25 mile	s = 0.5 mile
July 18, 1960												
1	290	[a]1.1	59.6	44.1	40.5	25.0		20.6	20.2		8.5	7.6
2	240	1.118	39.5	51.5	40.4	33.2		22.8	20.0		8.2	6.3
3	210	[a]1.13	78.7	57.3	52.2	50.0		29.3	33.2		7.9	7.9
4	320	[a]1.14	57.9	42.5	34.1	35.1		17.5	21.1		10.3	8.6
5	50	1.12	229.3	153.7	84.1	95.7		39.7			4.4	2.9
6	280	1.119	62.6	46.2	25.8	36.8		19.3	22.2		10.3	5.0
7	890	[a]1.12	26.1	20.4		16.0			9.2		3.9	3.3
July 20, 1960												
14	305	1.163	61.2	45.0	46.2	44.9	61.1	24.1		13.1	15.2	
15	250	1.155	70.7	51.0	50.8	48.8	61.7	25.3		13.5	8.5	
16	110	1.130	128.1	89.9	79.3	98.8	120.1	50.5		18.0	14.3	
17	[a]300	[a]1.16				32.7	48.9			14.6	15.9	
18	260	1.136	64.4	49.3	50.7	47.5	68.0	25.8		13.1	12.5	
19	125	1.116	114.7	80.6	65.8	71.9	95.7	39.5		13.9	15.4	

[a]Estimated value.

TABLE IV.- COMPARISON OF CALCULATED AND

MEASURED TIME INTERVALS

(a) Airplane A

Flight test	Altitude, ft	Mach number	Velocity, V, ft/sec	$\Delta t = \frac{l}{V}$, sec	Δt, sec, at -					
					s = 0		s = -0.2 mile		s = 0.25 mile	
					Eq. (3) of ref. 1	Measured	Eq. (3) of ref. 1	Measured	Eq. (3) of ref. 1	Measured
July 19, 1960										
8	380	1.053	1,210	0.046	0.053	0.056	0.070	0.065	0.074	0.068
9	200	1.065	1,226	.045	.042	.049	.065	.057	.068	.062
10	140	1.074	1,237	.044	.037	.049	.062	-----	.065	-----
11	330	1.074	1,229	.045	.046	.053	.063	.061	.066	.065
12	340	1.145	1,304	.042	.039	.053	.052	.051	.054	.057
13	110	1.149	1,322	.042	.028	.047	.050	.057	.053	.059
July 21, 1960										
20	485	1.077	1,277	0.043	0.049	0.050	0.061	0.054		
21	270	1.092	1,271	.043	.041	.049	.057	.051		
22	60	1.124	1,268	.043	.026	.047	.054	-----		
23	590	1.065	1,226	.045	.046	.057	.055	.063		
24	190	1.068	1,226	.045	.035	.047	.054	.057		
25	95	1.088	1,243	.044	.028	.050	.052	-----		

TABLE IV.- COMPARISON OF CALCULATED AND

MEASURED TIME INTERVALS - Concluded

(b) Airplane B

Flight test	Altitude, ft	Mach number	Velocity, V, ft/sec	$\Delta t = \frac{l}{V}$, sec	Δt, sec, at -							
					s = 0		s = -0.2 mile		s = 0.25 mile		s = 0.5 mile	
					Eq. (3) of ref. 1	Measured	Eq. (3) of ref. 1	Measured	Eq. (3) of ref. 1	Measured	Eq. (3) of ref. 1	Measured
July 18, 1960												
1	290	[a]1.1	1,250	0.050	0.046	0.063			0.067	0.072	0.079	0.074
2	240	1.118	1,274	.049	.041	.061			.064	.071	.075	.079
3	210	[a]1.13	1,285	.049	.039	.059			.062	.072	.073	.079
4	320	[a]1.14	1,294	.049	.042	.057			.061	.072	.072	.076
5	50	1.12	1,274	.049	.028	.057			.063	.086	.075	.095
6	280	1.119	1,275	.049	.043	.0615			.064	.072	.075	-----
7	890	[a]1.12	1,274	.049	.057	.064			.066	-----	.076	-----
July 20, 1961												
14	305	1.163	1,325	0.047	0.040	0.058	0.055	0.067	0.058	0.069		
15	250	1.155	1,351	.047	.038	.058	.054	.065	.057	.067		
16	110	1.130	1,310	.048	.033	.054	.057	.067	.061	-----		
17	[a]300	[a]1.16	1,319	-----	-----	-----	-----	.067	-----	-----		
18	260	1.136	1,316	.048	.040	.059	.057	.066	.060	.068		
19	125	1.116	1,265	.050	.036	.059	.061	.063	.064	.066		

[a]Estimated value.

TABLE V.- SUMMARY OF WINDOW DATA

(a) Airplane B; July 18, 1960

Window test location (a)	Summary of data for airplane flight test - 1			2			3			4			5			6			7		
	Estimated Δp_o, lb/sq ft	Window type (b)	Damage	Estimated Δp_o, lb/sq ft	Window type (b)	Damage	Estimated Δp_o, lb/sq ft	Window type (b)	Damage	Estimated Δp_o, lb/sq ft	Window type (b)	Damage	Estimated Δp_o, lb/sq ft	Window type (b)	Damage	Estimated Δp_o, lb/sq ft	Window type (b)	Damage	Estimated Δp_o, lb/sq ft	Window type (b)	Damage
1	32	P	No	35	P	No	51	P	No	35	P	No	90	P	Yes	31			16		
2	32	C	No	35	C	No	51	C	No	35	C	No	90	C	Yes	31			16		
3	30	P	No	32	P	No	45	P	No	33	P	No	67	P	No	28	P	No	14	P	No
4	30	C	No	32	C	No	45	C	No	33	C	No	67	C	No	28	C	No	14	C	No
5	28	P	No	27	P	No	33	P	No	30	P	No	50	P	No	26	P	No	12	P	No
6	28	C	No	27	C	No	33	C	No	30	C	No	50	C	No	26	C	No	12	C	No
7	20	P	No	23	P	No	24	P	No	25	P	No	35	P	No	16	P	No	10	P	No
8	20	C	No	23	C	No	24	C	No	25	C	No	35	C	No	16	C	No	10	C	No
9	14	P	No	13	P	No	16	P	No	15	P	No	15	P	No	10	P	No	5	P	No
10	14	C	No	13	C	No	16	C	No	15	C	No	15	C	No	10	C	No	5	C	No

(b) Airplane A; July 19, 1960

Window test location (a)	Summary of data for airplane flight test - 8			9			10			11			12			13		
	Estimated Δp_o, lb/sq ft	Window type (b)	Damage	Estimated Δp_o, lb/sq ft	Window type (b)	Damage	Estimated Δp_o, lb/sq ft	Window type (b)	Damage	Estimated Δp_o, lb/sq ft	Window type (b)	Damage	Estimated Δp_o, lb/sq ft	Window type (b)	Damage	Estimated Δp_o, lb/sq ft	Window type (b)	Damage
1	23	P	Yes	29			30	P	No	23	P	No	24	C	Yes	30		
2	33	P	No	56	P	Yes	77			38			42	P	No	72	P	Yes
3	33	P	Yes	56	P	Yes	77	P	Yes	38			42	C	No	72	C	Yes
4	33	P	No	56	P	Yes	77			38			42	P	No	72	P	Yes
5	33	P	No	56	P	Yes	77			38			42	C	No	72	C	No
6	24	P	Yes	30	P	Yes	32	P	No	24	P	Yes	25	C	Yes	32		
7	33	P	No	56	P	Yes	77			38			42	P	Yes	72		
8	26	P	No	34	P	Yes	40			26			27			36		
9	33	P	No	56	P	Yes	77			38			42	C	No	72	C	Yes
10	25	P	Yes	32	P	Yes	34	P	Yes	25			26	C	Yes	34		

[a] See figure 9 for schematic representation of window test locations.

[b] The letter P represents plain windows; the letter C, colonial windows.

TABLE V.- SUMMARY OF WINDOW DATA - Concluded

(c) Airplane B; July 20, 1960

Window test location (a)	Summary of data for airplane flight test - 14			15			16			17			18			19		
	Estimated Δp_o, lb/sq ft	Window type (b)	Damage	Estimated Δp_o, lb/sq ft	Window type (b)	Damage	Estimated Δp_o, lb/sq ft	Window type (b)	Damage	Estimated Δp_o, lb/sq ft	Window type (b)	Damage	Estimated Δp_o, lb/sq ft	Window type (b)	Damage	Estimated Δp_o, lb/sq ft	Window type (b)	Damage
1	50	C	No	52	C	No	93	C	Yes	37	C	No	52	C	No	73	C	Yes
2		C	No		C	No		C	No		C	No		C	No		C	No
3		C	No		C	No		C	No		C	No		C	No		C	No
4		C	No		C	No		C	No		C	No		C	No		C	No
5		C	No		C	No		C	Yes		C	No		C	No		C	No
6		C	No		C	No		C	No		C	No		C	No		C	Yes
7		C	No		C	No		C	No		C	No		C	No		C	Yes
8		C	No		C	No		C	Yes		C	No		C	No		C	Yes
9		C	No		C	No		C	No		C	No		C	No		C	No
10		C	No		C	No		C	Yes									

(d) Airplane A; July 21, 1960

Window test location (a)	Summary of data for airplane flight test - 20			21			22			23			24			25		
	Estimated Δp_o, lb/sq ft	Window type (b)	Damage	Estimated Δp_o, lb/sq ft	Window type (b)	Damage	Estimated Δp_o, lb/sq ft	Window type (b)	Damage	Estimated Δp_o, lb/sq ft	Window type (b)	Damage	Estimated Δp_o, lb/sq ft	Window type (b)	Damage	Estimated Δp_o, lb/sq ft	Window type (b)	Damage
1	30	P	No	48	P	No	94	P	Yes	24	C	No	62	C	Yes	86		
2		P	No		P	No		P	Yes		C	No		C	No		C	No
3		P	No		P	No		P	Yes		C	No		C	No		C	No
4		P	No		P	No		P	Yes		C	No		C	No		C	Yes
5		P	No		P	No		P	Yes		C	No		C	No		C	No
6		P	No		P	Yes					C	No		C	Yes			
7		P	No		P	No		P	Yes		C	No		C	No		C	Yes
8		P	No		P	Yes					C	No		C	Yes			
9		P	No		P	Yes					C	No		C	No		C	Yes
10		P	No		P	Yes					C	No		C	Yes			

[a] See figure 9 for schematic representation of window test locations.

[b] The letter P represents plain windows; the letter C, colonial windows.

TABLE VI.- SHOCK-WAVE ANGLES

Flight test	Mach number	Altitude, ft	Mach angle, $\sin^{-1}\left(\frac{1}{M}\right)$, deg	μ_{exp}, deg
Airplane B; July 18, 1960				
1	[a]1.1	290		
2	1.118	240	63.43	62.97
3	[a]1.13	210		
4	[a]1.14	320		
5	1.12	50	63.25	64.11
6	1.119	280	63.37	63.14
7	[a]1.12	890		
Airplane A; July 19, 1960				
8	1.053	380	70.65	67.04
9	1.065	200	68.18	69.04
10	1.074	140	66.58	67.32
11	1.074	330	67.95	67.49
12	1.145	340	60.85	60.28
13	1.149	110	59.13	60.68
Airplane B; July 20, 1960				
14	1.163	305	59.30	60.62
15	1.155	250	59.99	59.07
16	1.130	110	62.22	62.34
17	[a]1.16	[a]300	-----	-----
18	1.136	260	59.87	59.19
19	1.116	125	63.65	63.88
Airplane A; July 21, 1960				
20	1.077	485	63.05	62.91
21	1.092	270	63.60	63.03
22	1.124	60	63.36	64.57
23	1.065	590	68.20	67.52
24	1.068	190	67.79	66.41
25	1.088	95	65.74	65.03

[a]Estimated value.

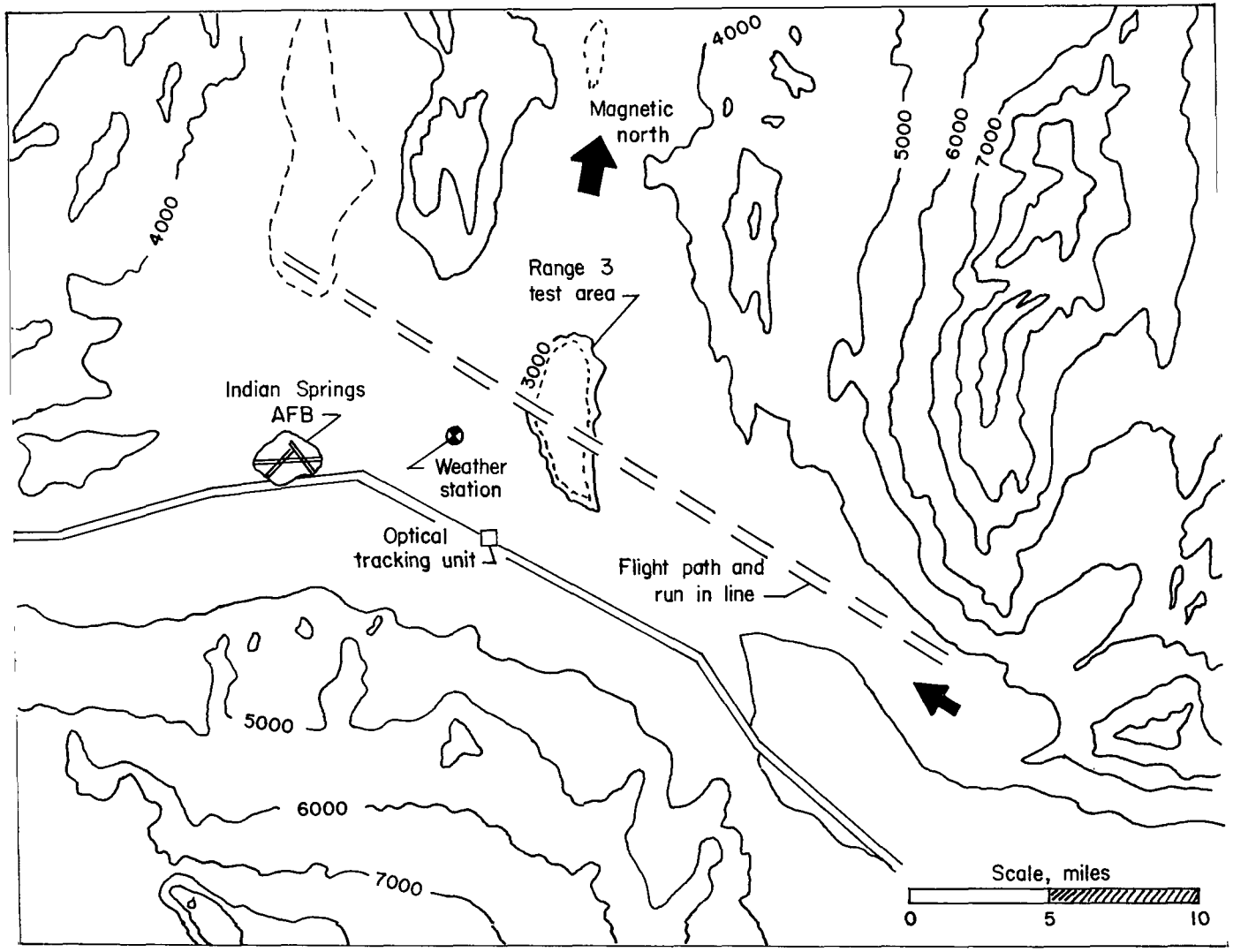

Figure 1.- Contour map showing test area, flight path, weather measuring station, and tracking unit.

L-61-5095

Figure 2.- Photograph of area in which tests were conducted. (Courtesy of U.S. Air Force.)

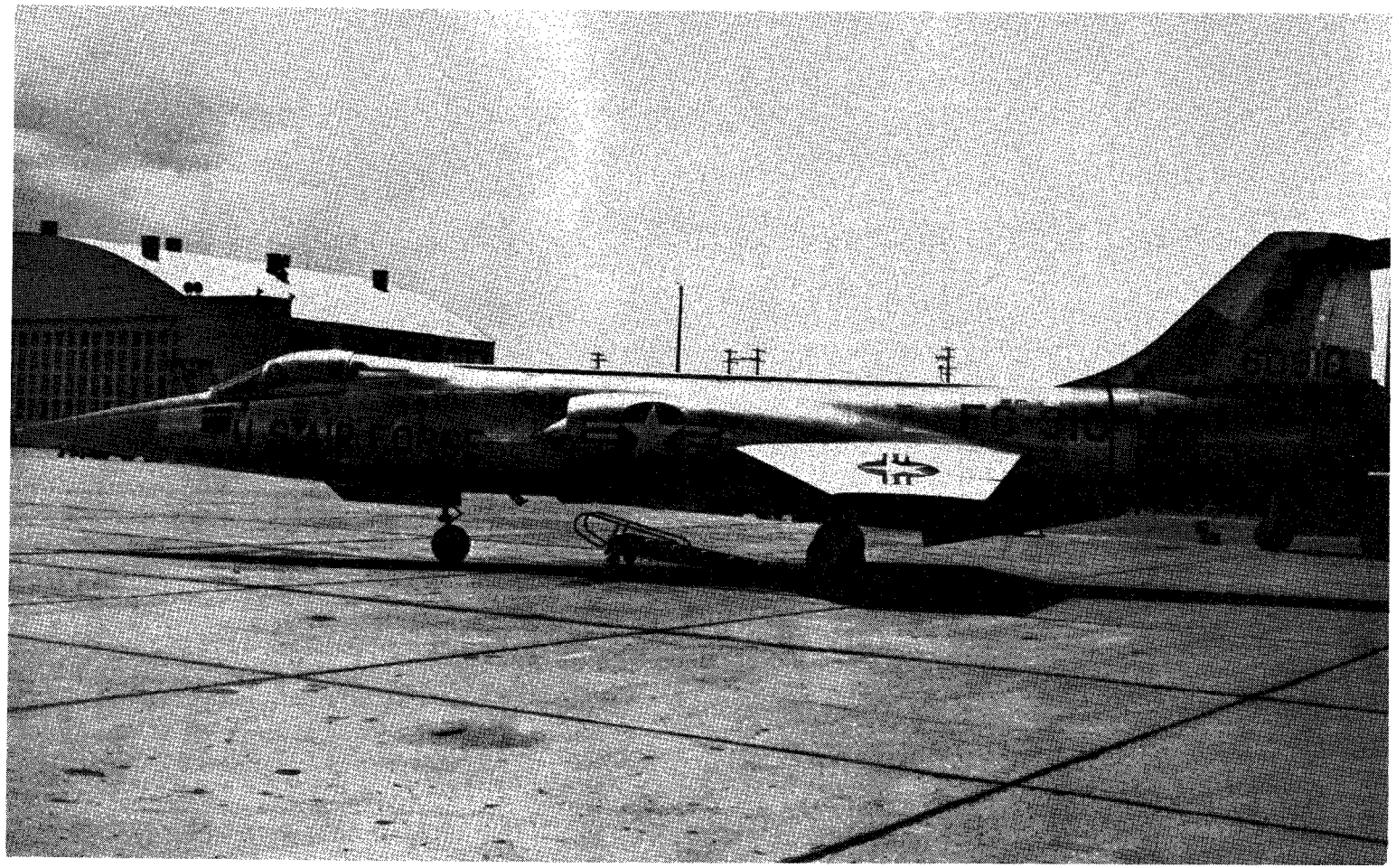

L-61-5096

(a) Side view.

Figure 3.- Photograph of airplane A. (Courtesy of U.S. Air Force.)

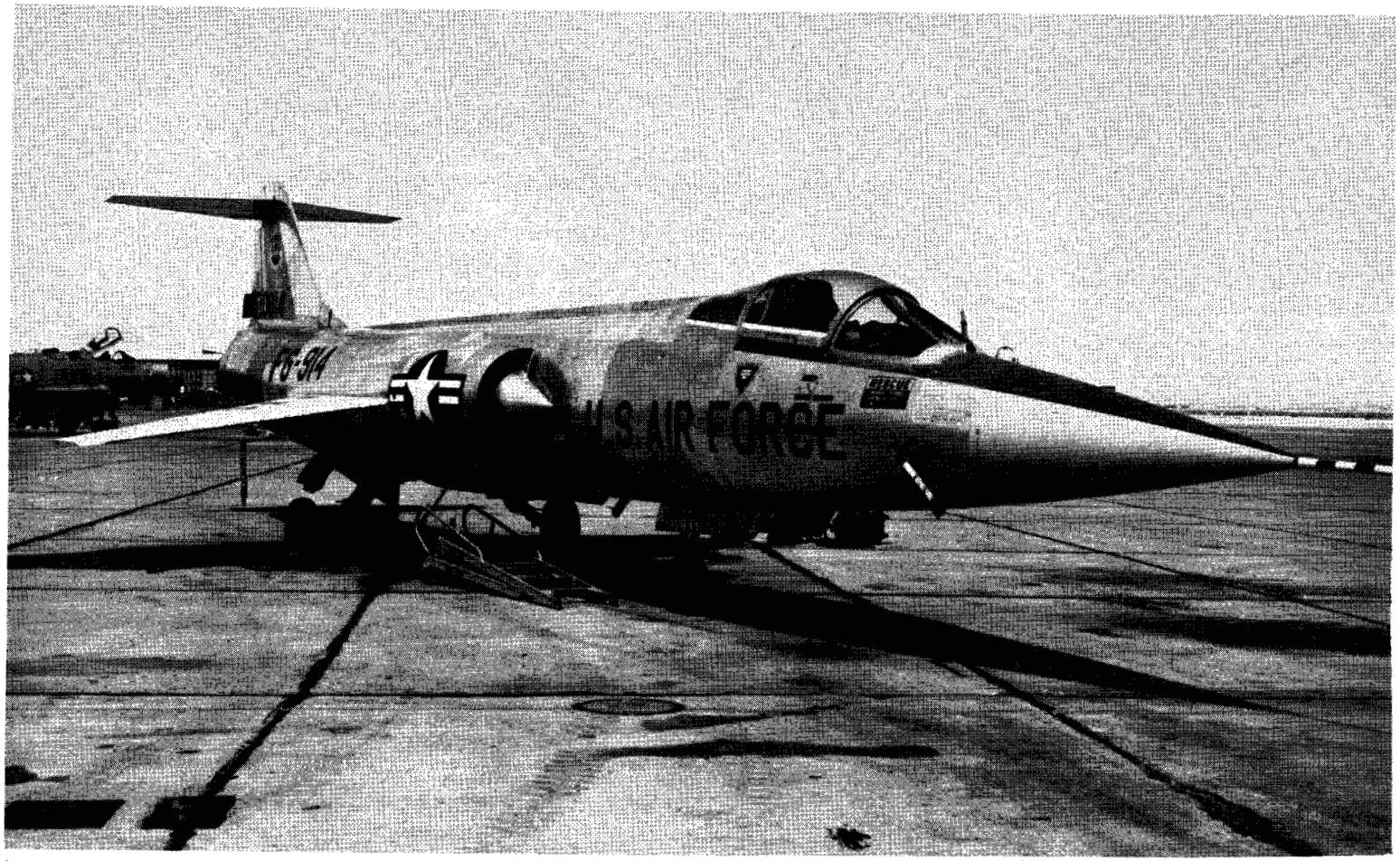

L-61-5097

(b) Three-quarter front view.

Figure 3.- Continued.

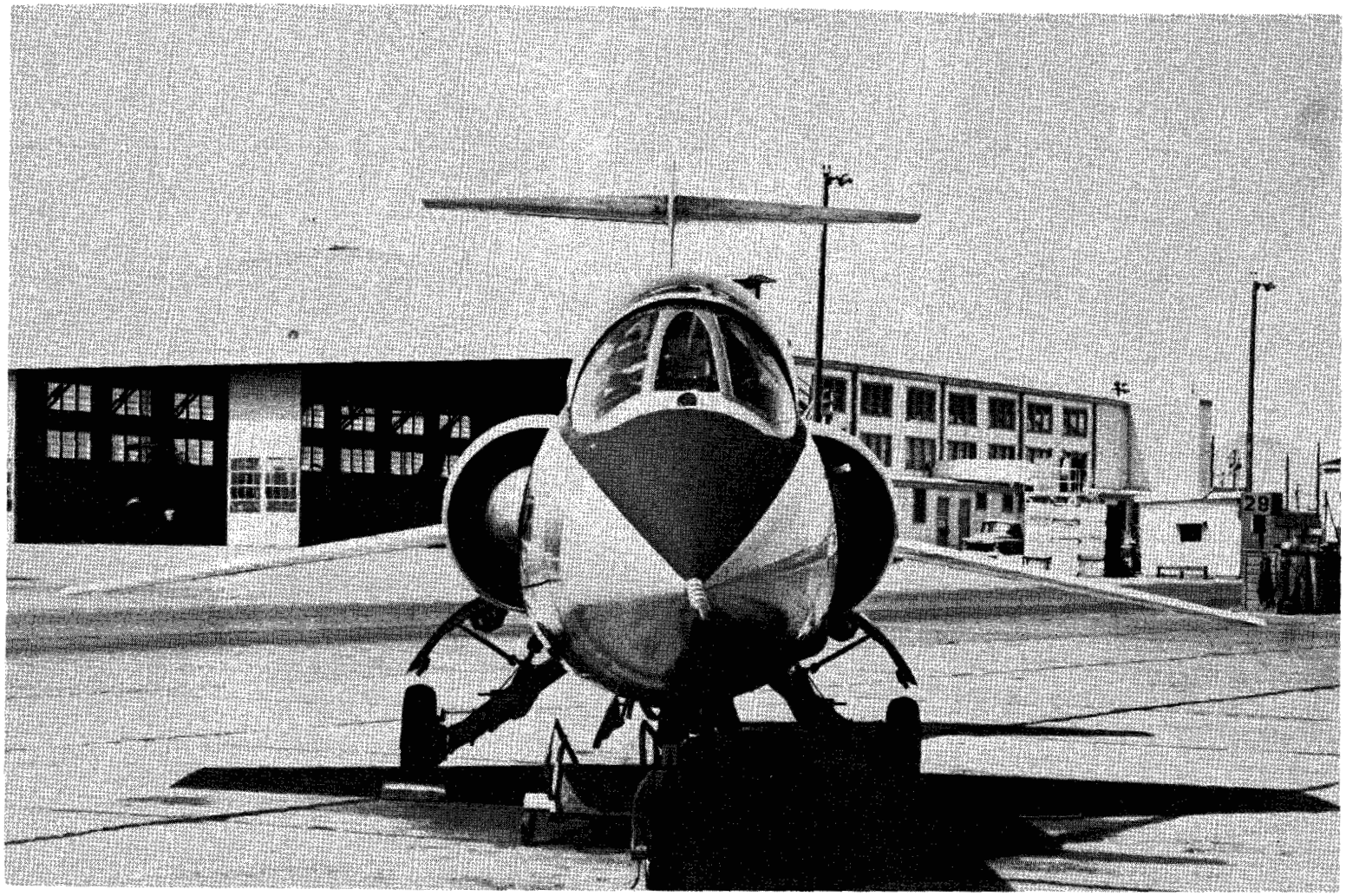

L-61-5098

(c) Front view.

Figure 3.- Concluded.

L-61-5099

(a) Side view.

Figure 4.- Photograph of airplane B. (Courtesy of U.S. Air Force.)

L-61-5100

(b) Three-quarter front view.

Figure 4.- Continued.

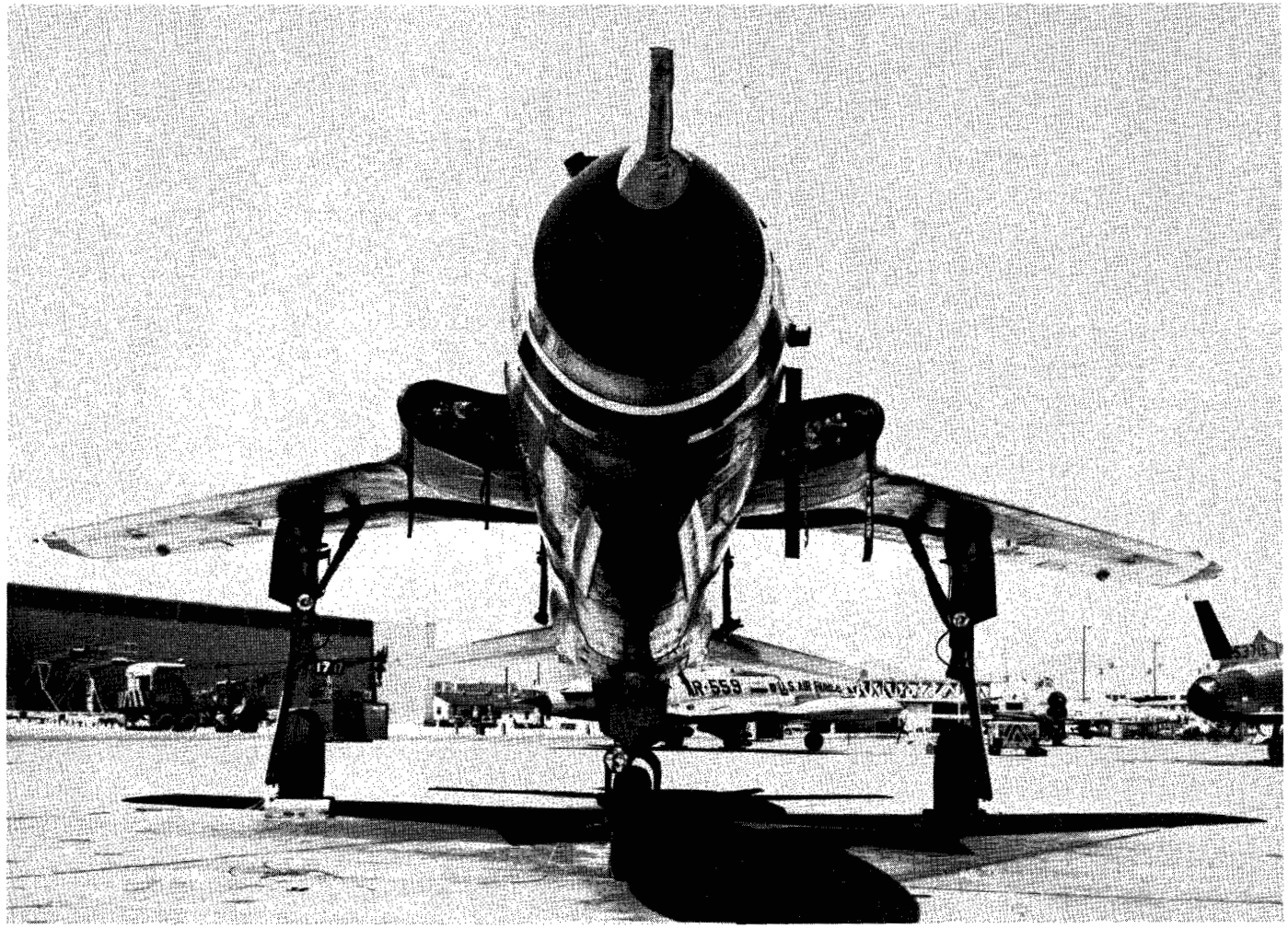

L-61-5101

(c) Front view.

Figure 4.- Concluded.

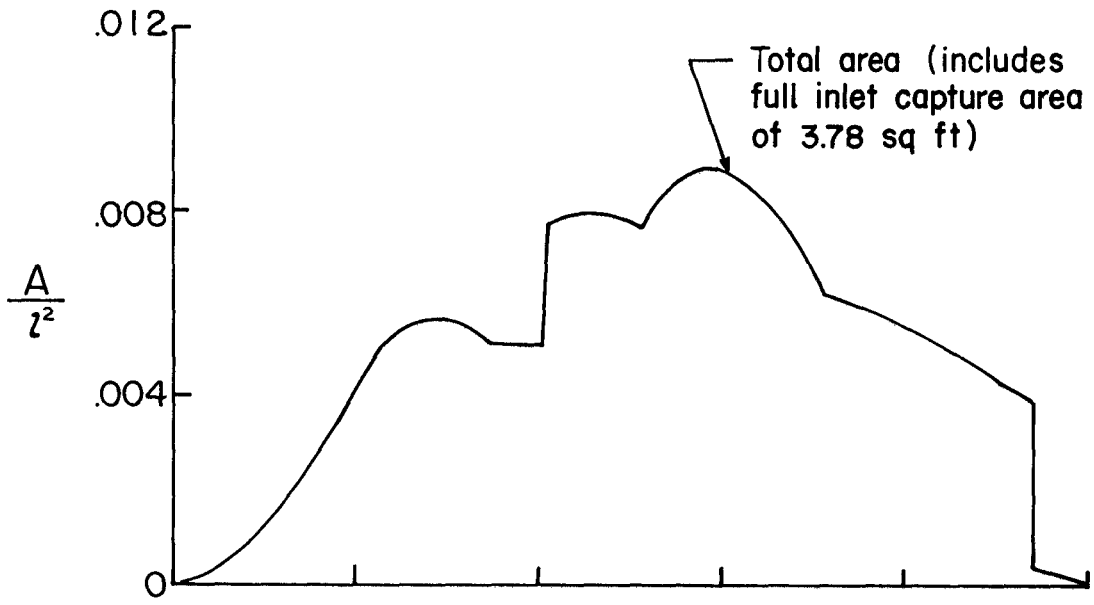

(a) Airplane A.

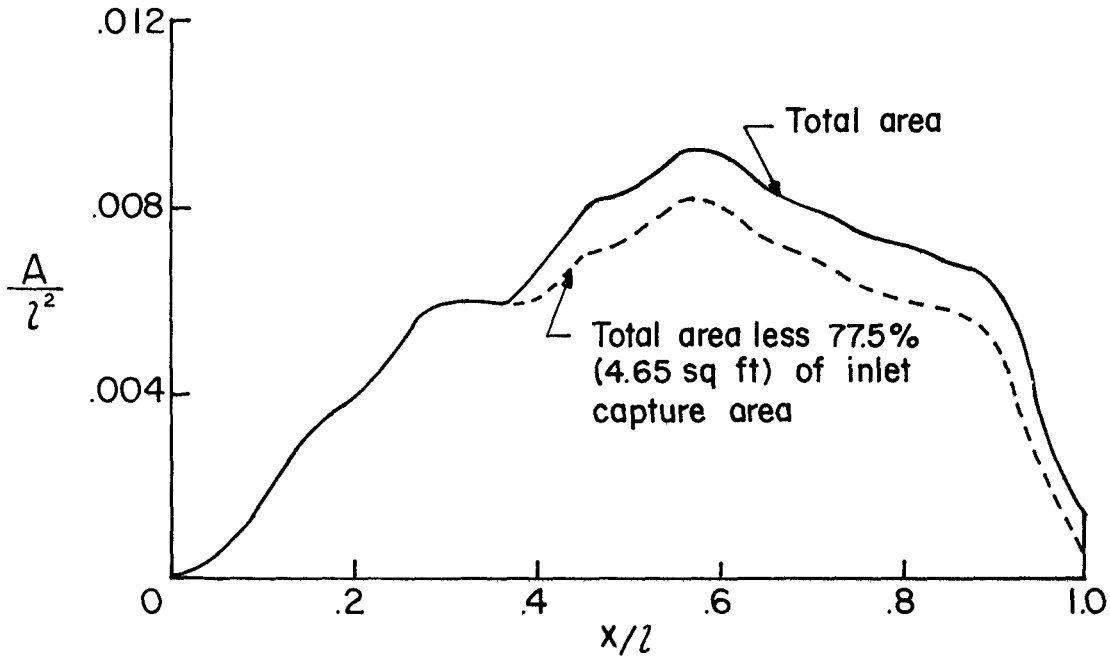

(b) Airplane B.

Figure 5.- Normal cross-sectional area distribution of test airplanes.

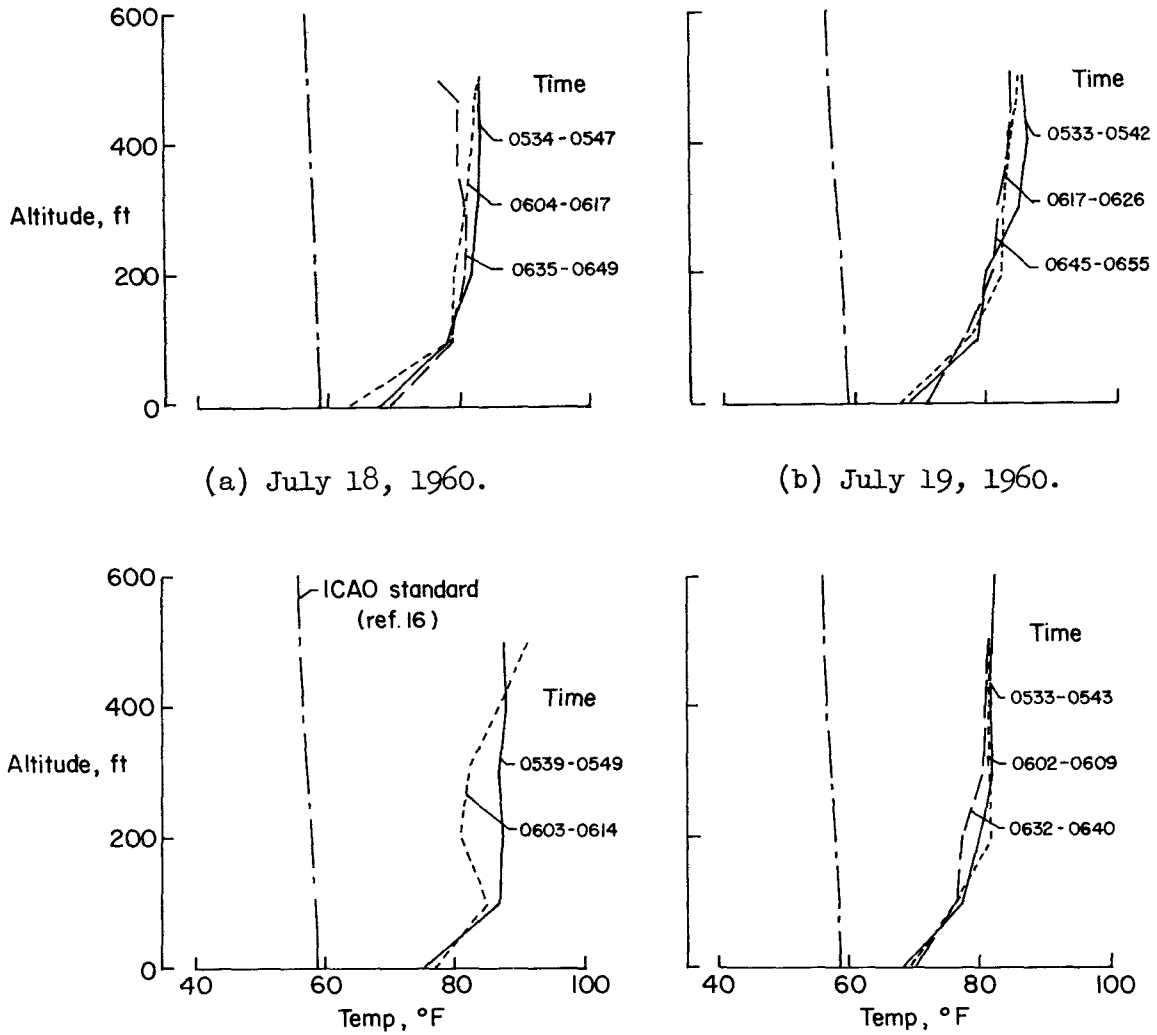

(a) July 18, 1960.

(b) July 19, 1960.

(c) July 20, 1960.

(d) July 21, 1960.

Figure 6.- Results from wiresonde atmospheric soundings taken during test flights.

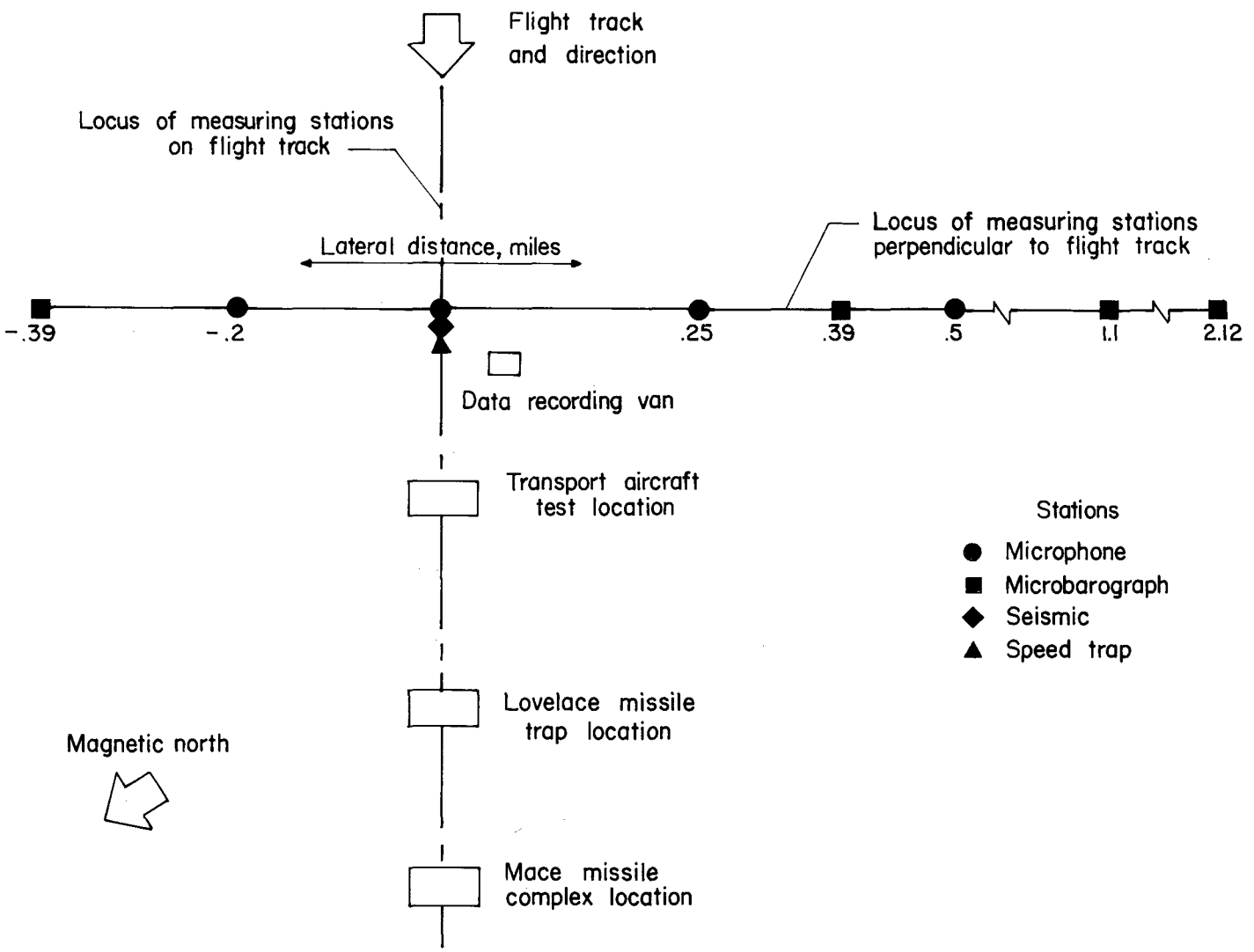

Figure 7.- Schematic diagram of instrument and equipment locations in test area.

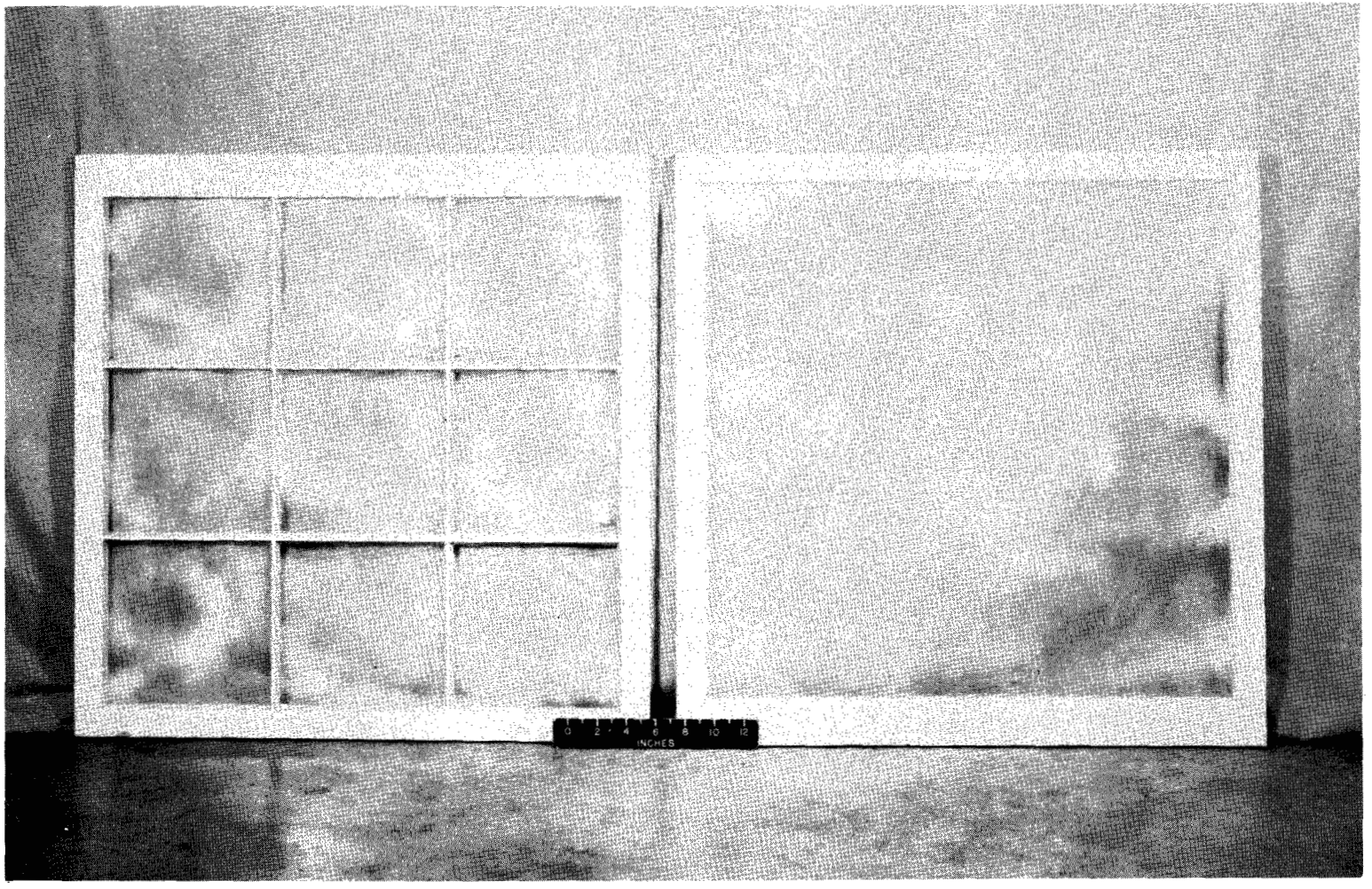

(a) Colonial and plain windows. L-61-379

Figure 8.- Photographs of two types of windows tested and test cubicle.

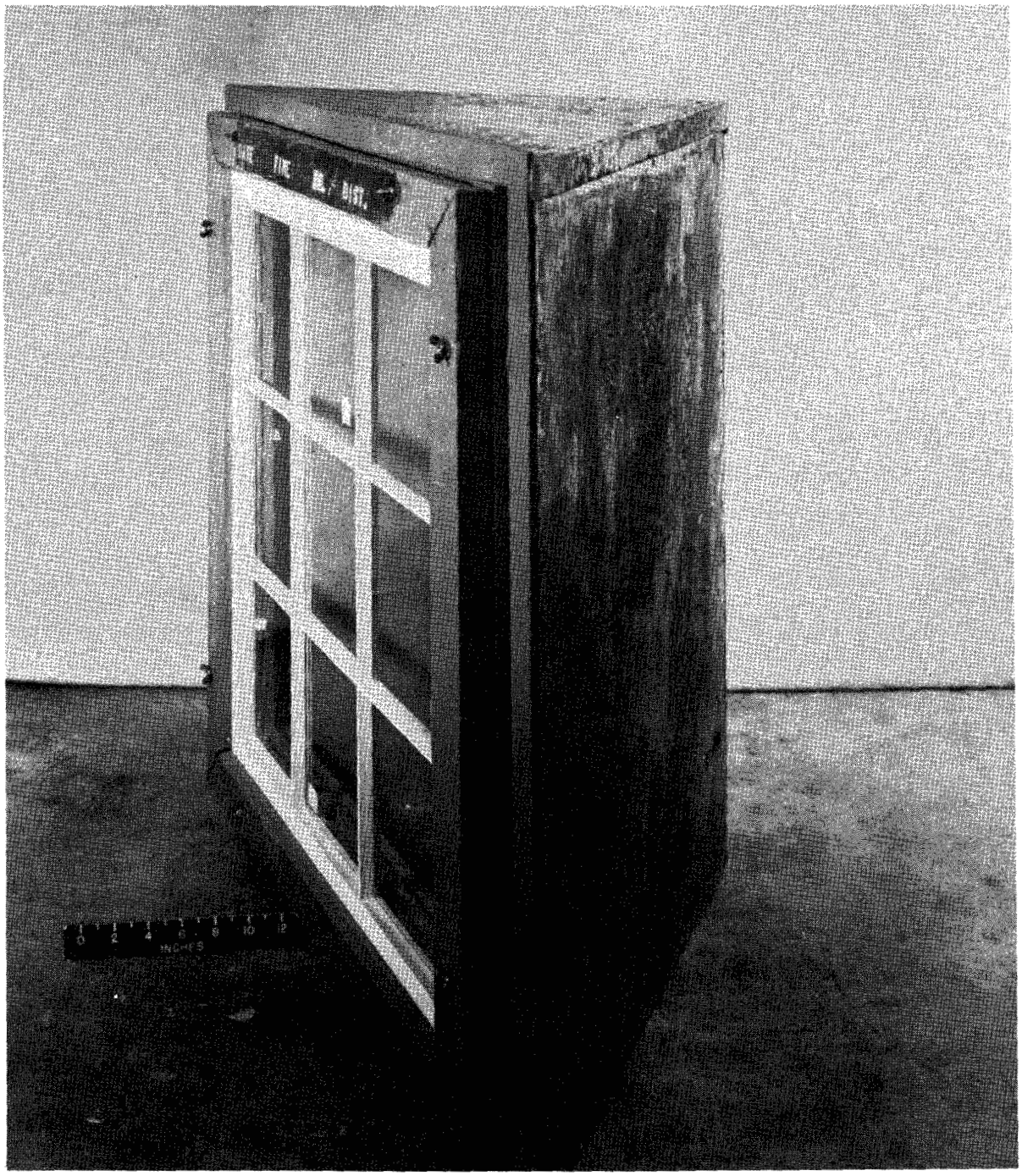

(b) Window cubicle. L-61-383

Figure 8.- Concluded.

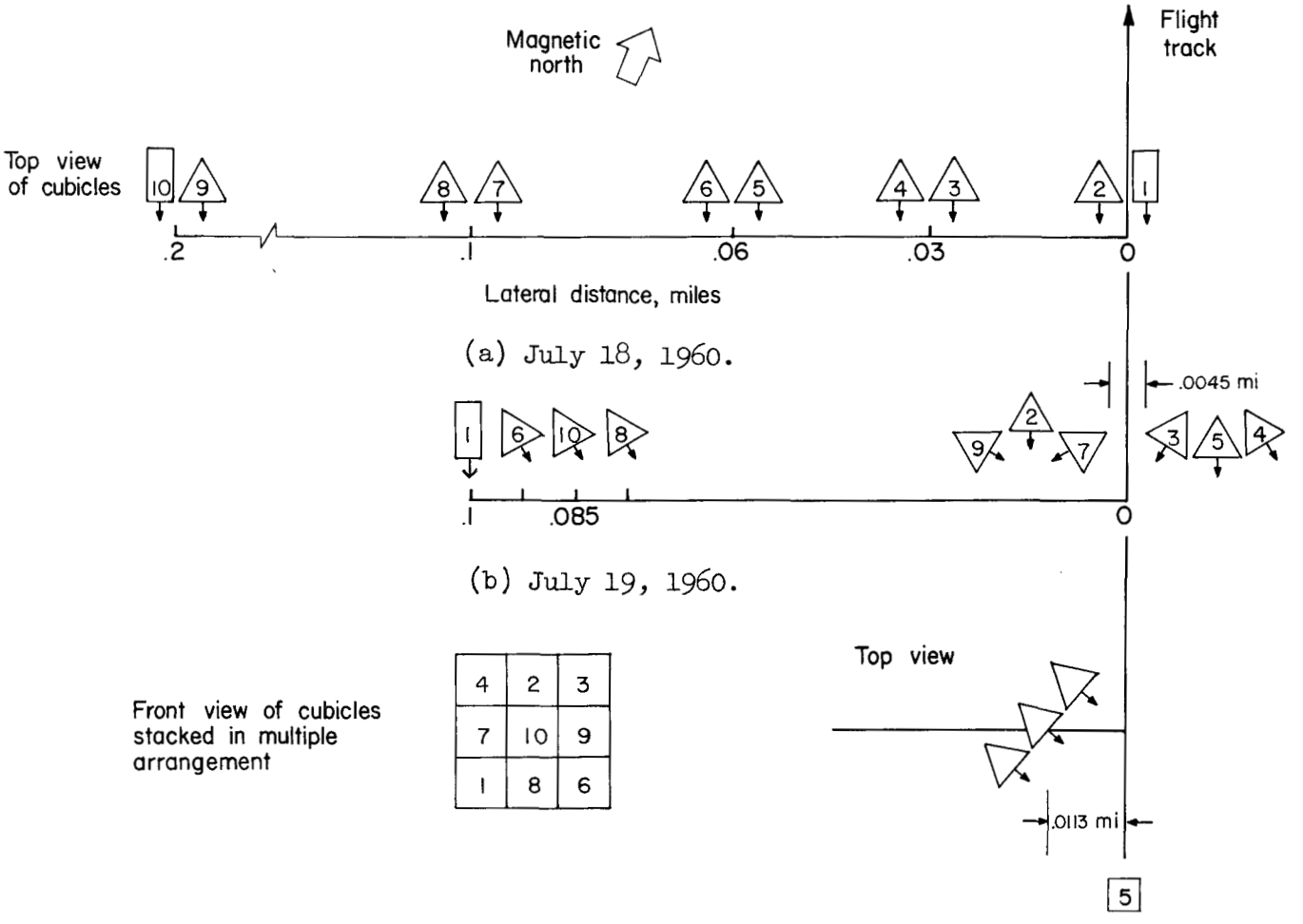

Figure 9.- Window test locations and orientations. (Directions of arrows on cubicles are perpendicular to glass.)

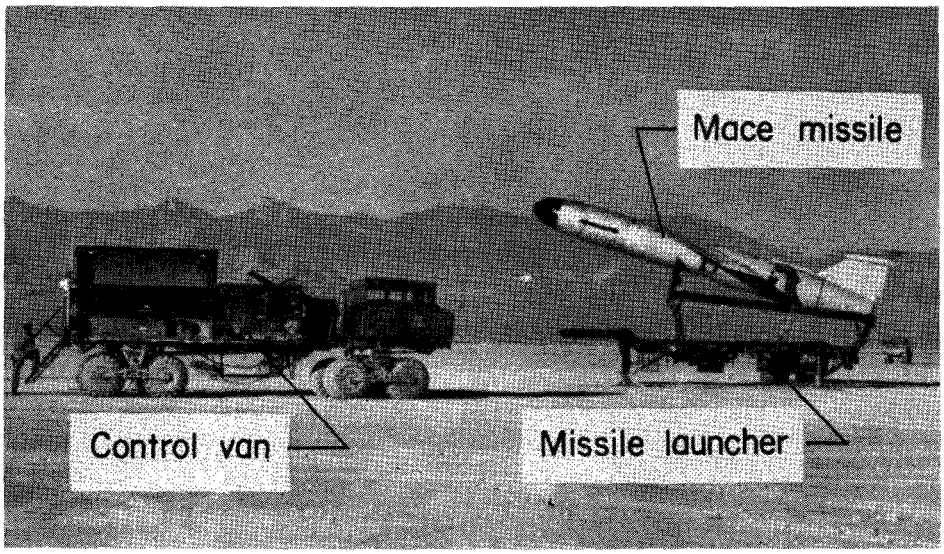

L-60-4992.1

Figure 10.- Photograph of Mace missile complex in test area.

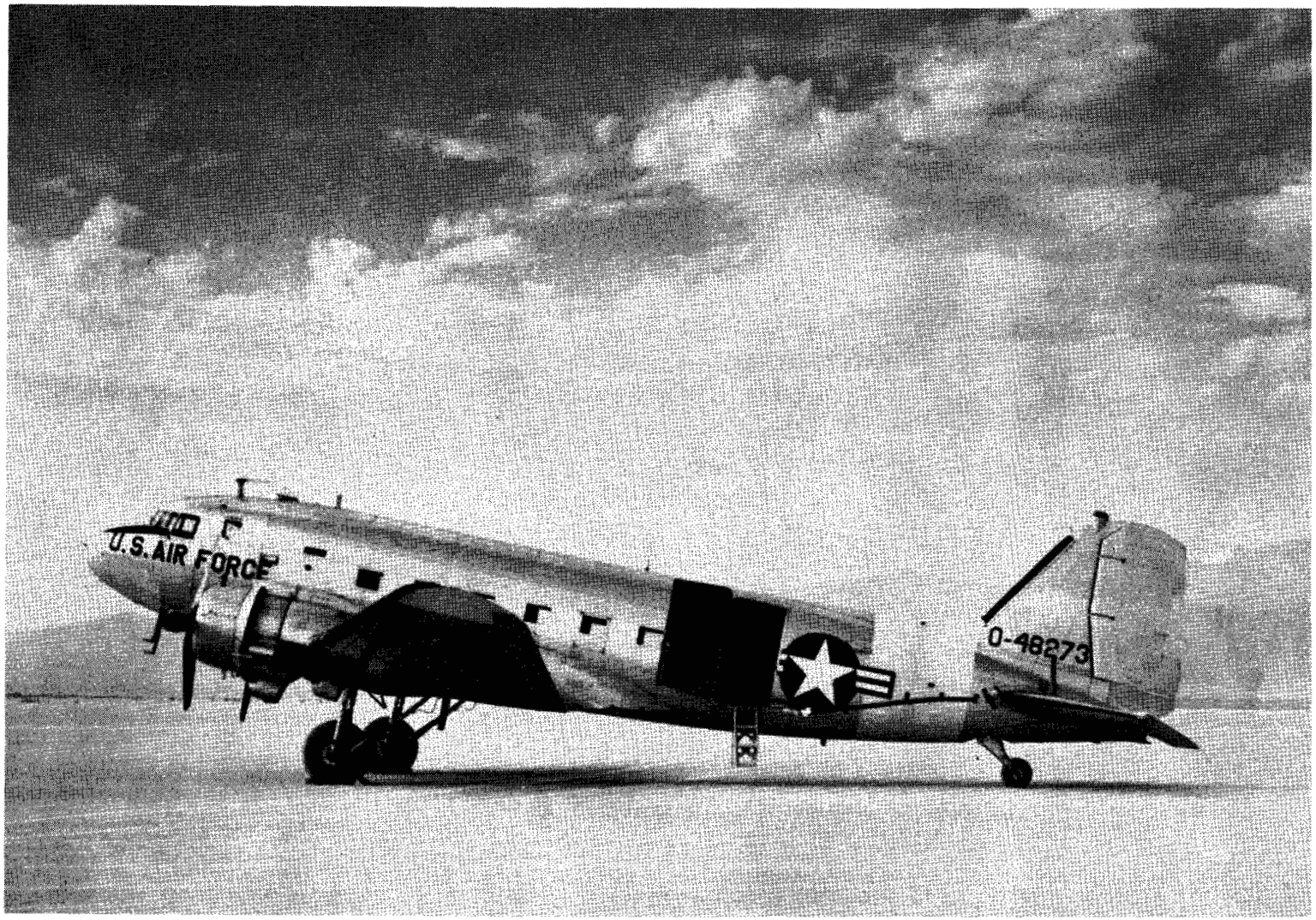

L-61-5102

Figure 11.- Photograph of transport aircraft for which structural-response tests were conducted.

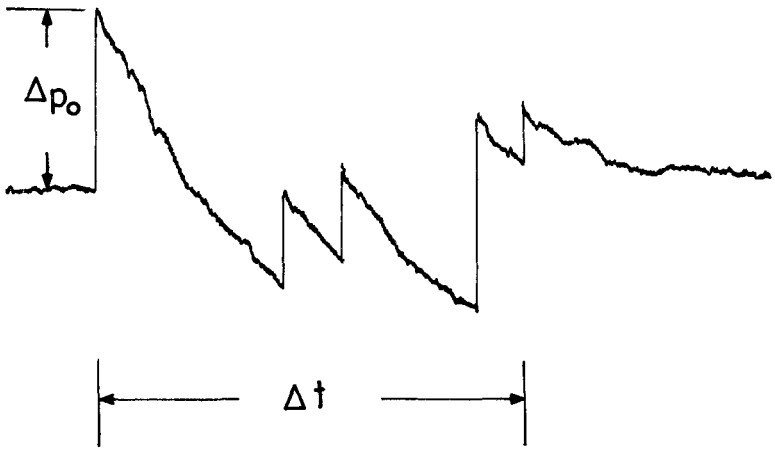

(a) Microphone at ground level.

(b) Microphone on top of 20-foot-high mast.

Figure 12.- Time histories of shock noise pressures from flight test 24 for airplane A.

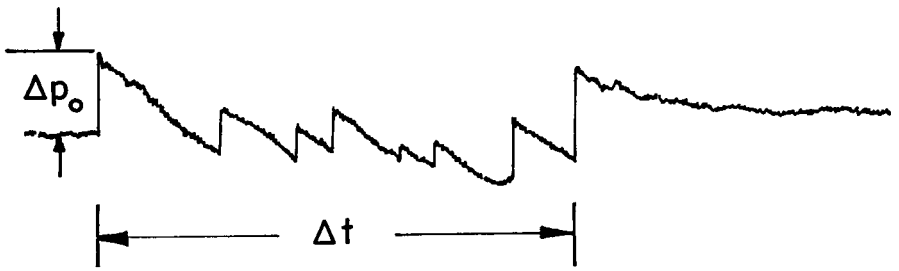

(a) Microphone at ground level.

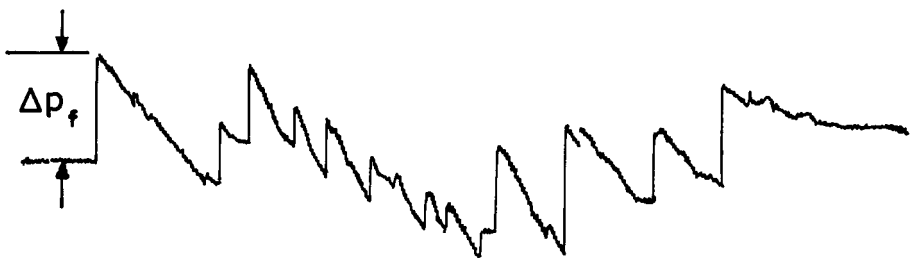

(b) Microphone on top of 20-foot-high mast.

Figure 13.- Time histories of shock noise pressures from flight test 15 for airplane B.

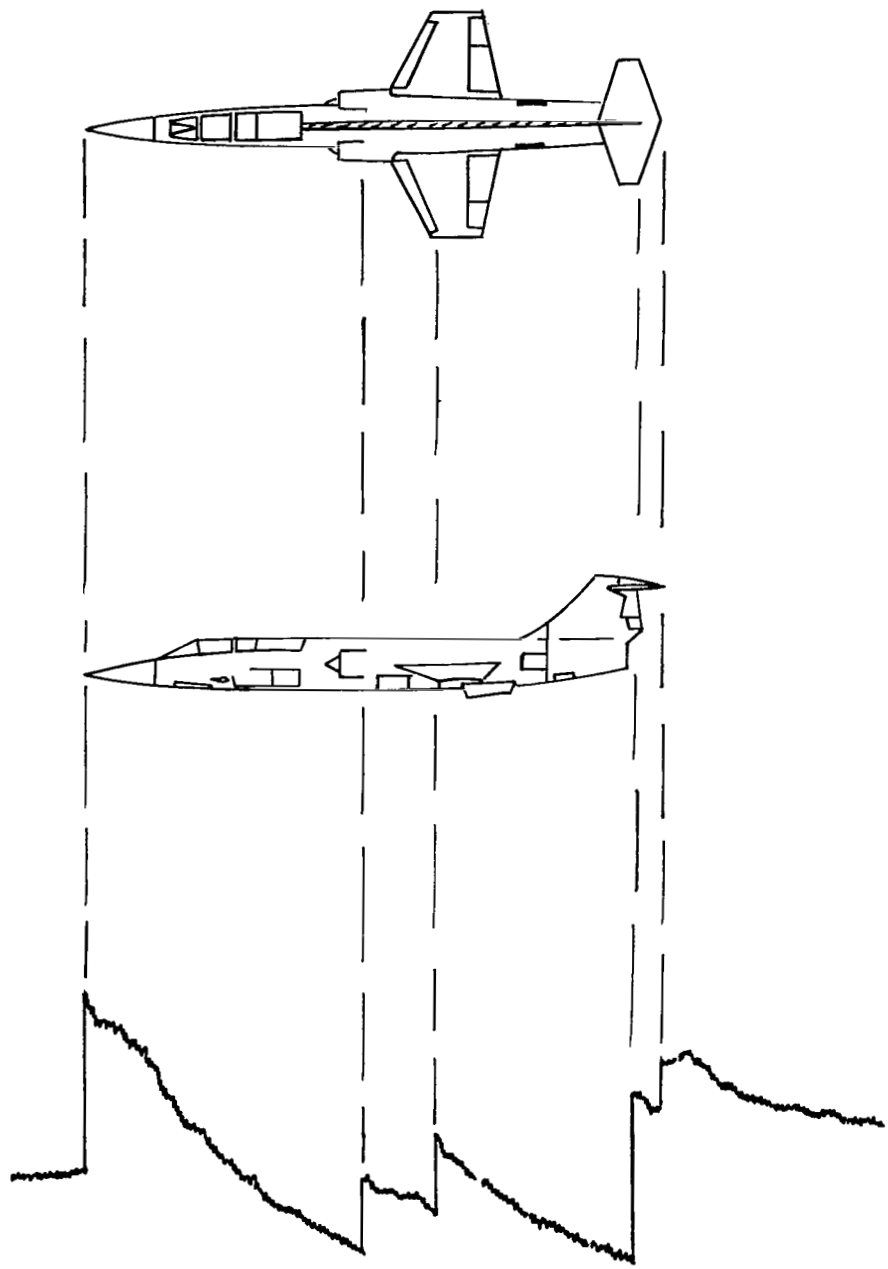

Figure 14.- Planform and side views of airplane A with a typical time history of shock noise pressure.

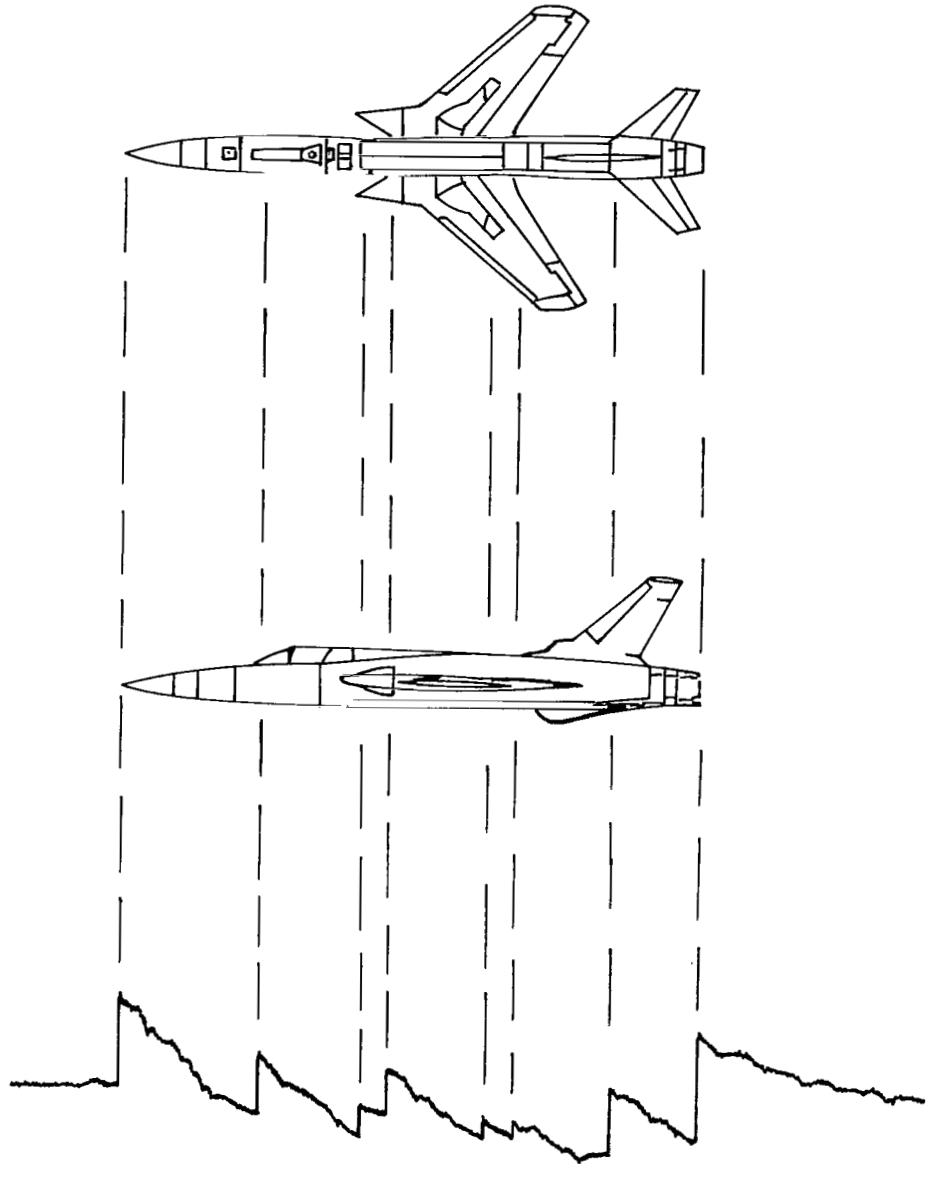

Figure 15.- Planform and side views of airplane B with a typical time history of shock noise pressure.

(a) Altitude = 60 feet; M = 1.124.

(b) Altitude = 95 feet; M = 1.088.

(c) Altitude = 190 feet; M = 1.068.

(d) Altitude = 340 feet; M = 1.145.

(e) Altitude = 590 feet; M = 1.065.

Figure 16.- Pressure time histories measured at the ground for airplane A at a range of altitudes from 60 to 590 feet.

(a) Altitude = 50 feet; M = 1.12.

(b) Altitude = 240 feet; M = 1.118.

(c) Altitude = 250 feet; M = 1.155.

(d) Altitude = 320 feet; M = 1.14.

Figure 17.- Pressure time histories measured at the ground for airplane B at a range of altitudes from 50 feet to 320 feet.

(a) Microphone at s = 0.

(b) Microphone at lateral distance of s = 0.25 mile.

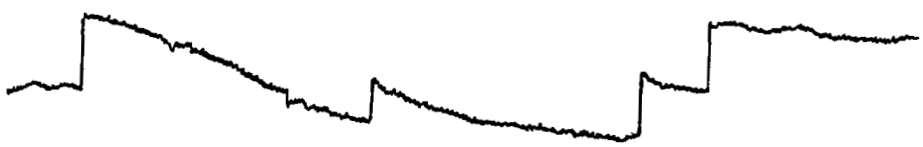

(c) Microphone at lateral distance of s = 0.5 mile.

Figure 18.- Pressure time histories measured at the ground for airplane B at various lateral distances from flight path. Altitude = 320 feet; M = 1.14.

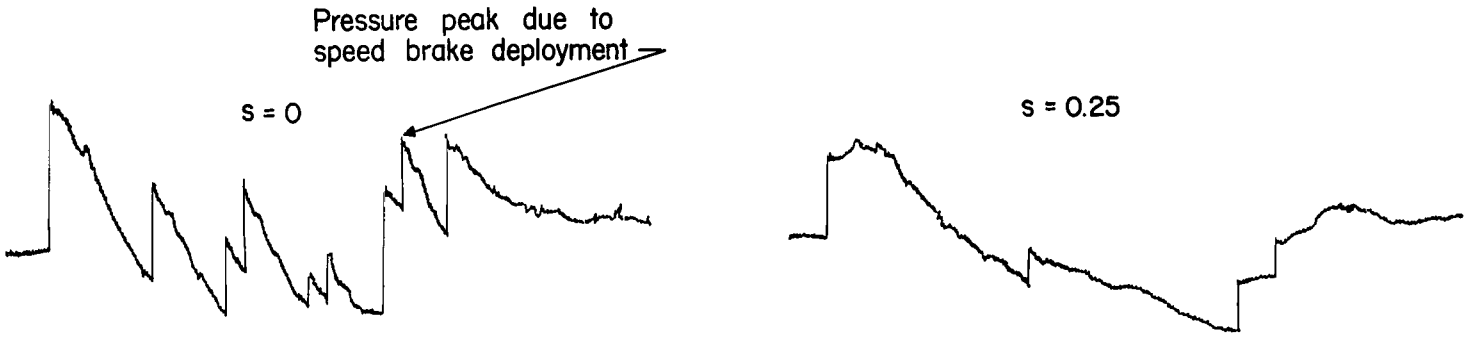

(a) Speed brakes deployed; altitude = 125 feet; M = 1.116.

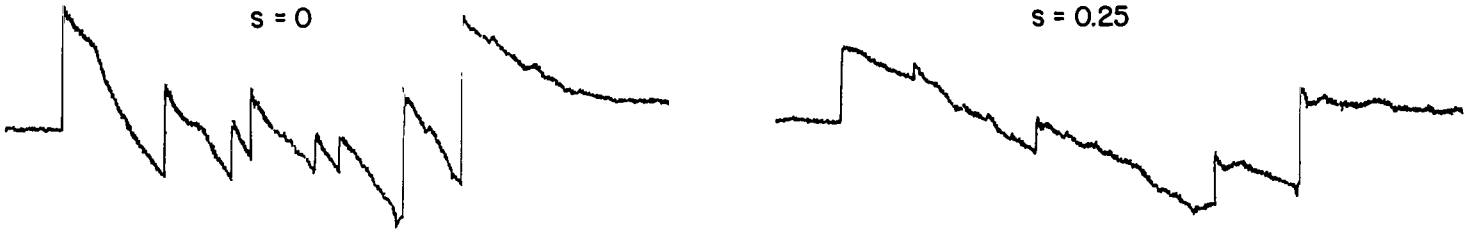

(b) Speed brakes in; altitude = 260 feet; M = 1.136.

Figure 19.- Pressure time histories measured on the ground for airplane B with and without speed brakes deployed.

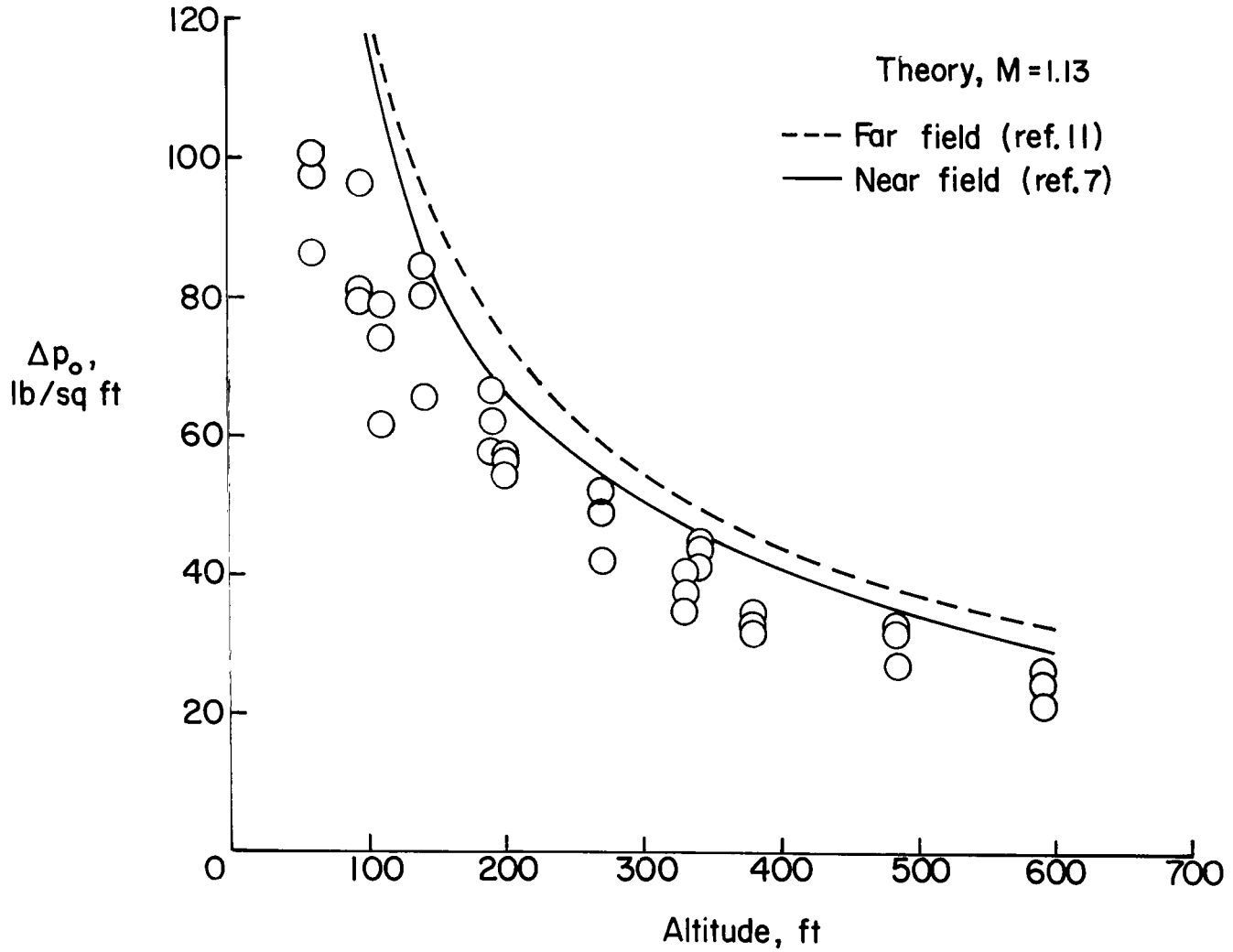

(a) Pressures measured at the ground.

Figure 20.- Measured and calculated variation with altitude of the shock-wave pressure along the flight path. Level flight of airplane A at Mach number from 1.053 to 1.149.

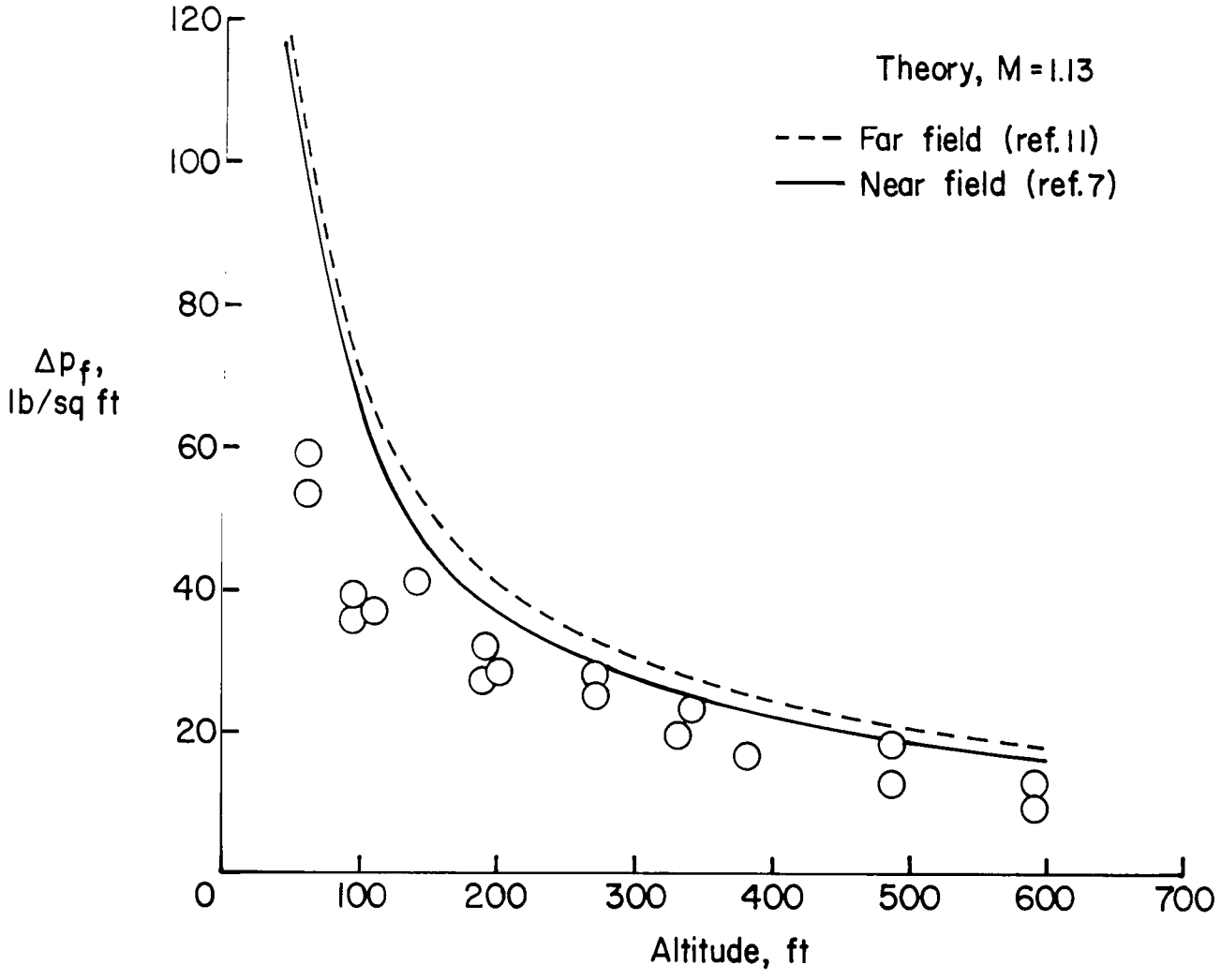

(b) Pressures measured in free air.

Figure 20.- Concluded.

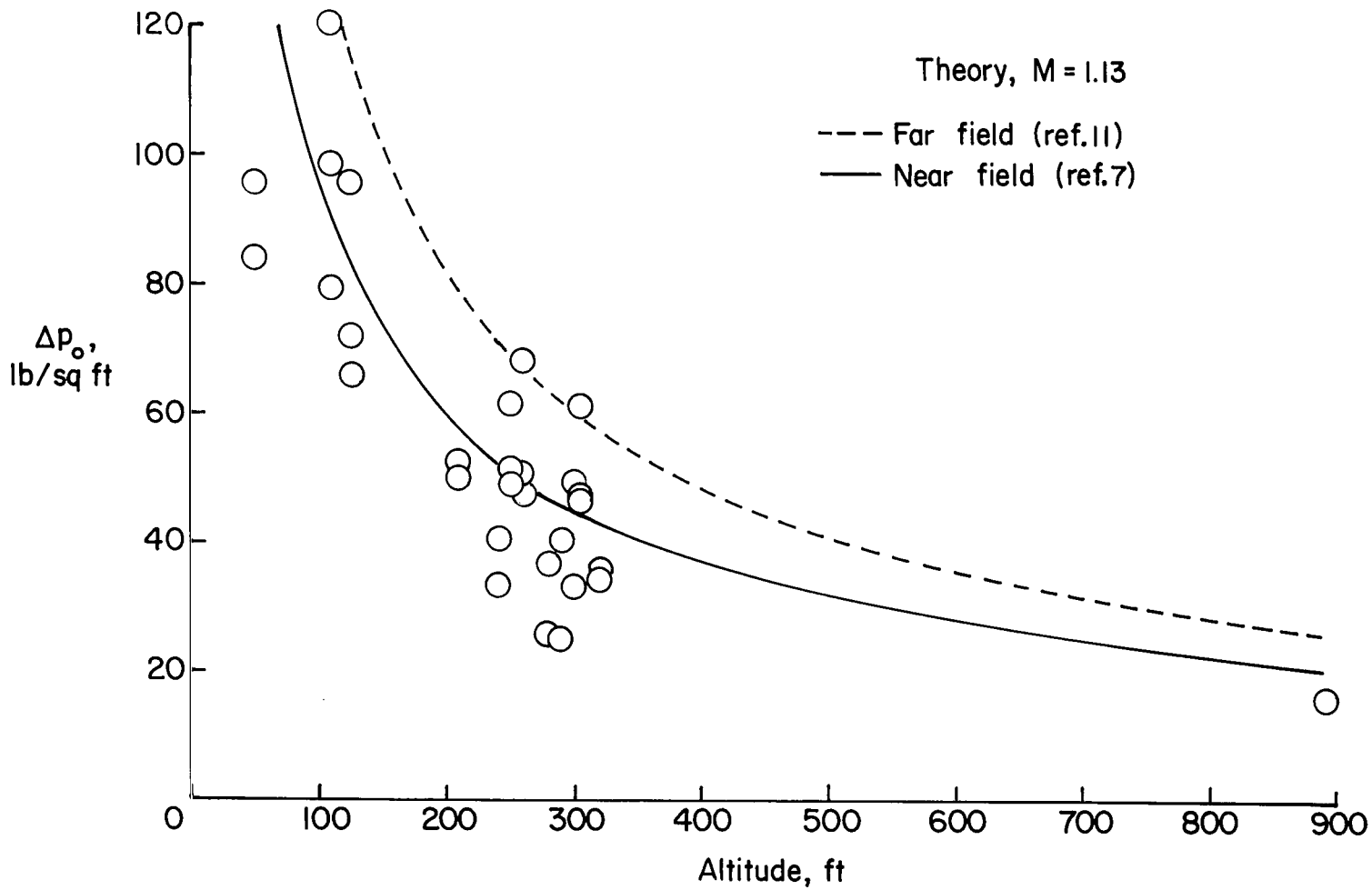

(a) Pressures measured at the ground.

Figure 21.- Measured and calculated variation with altitude of the shock-wave pressure along the flight path. Level flight of airplane B at Mach number from 1.10 to 1.163.

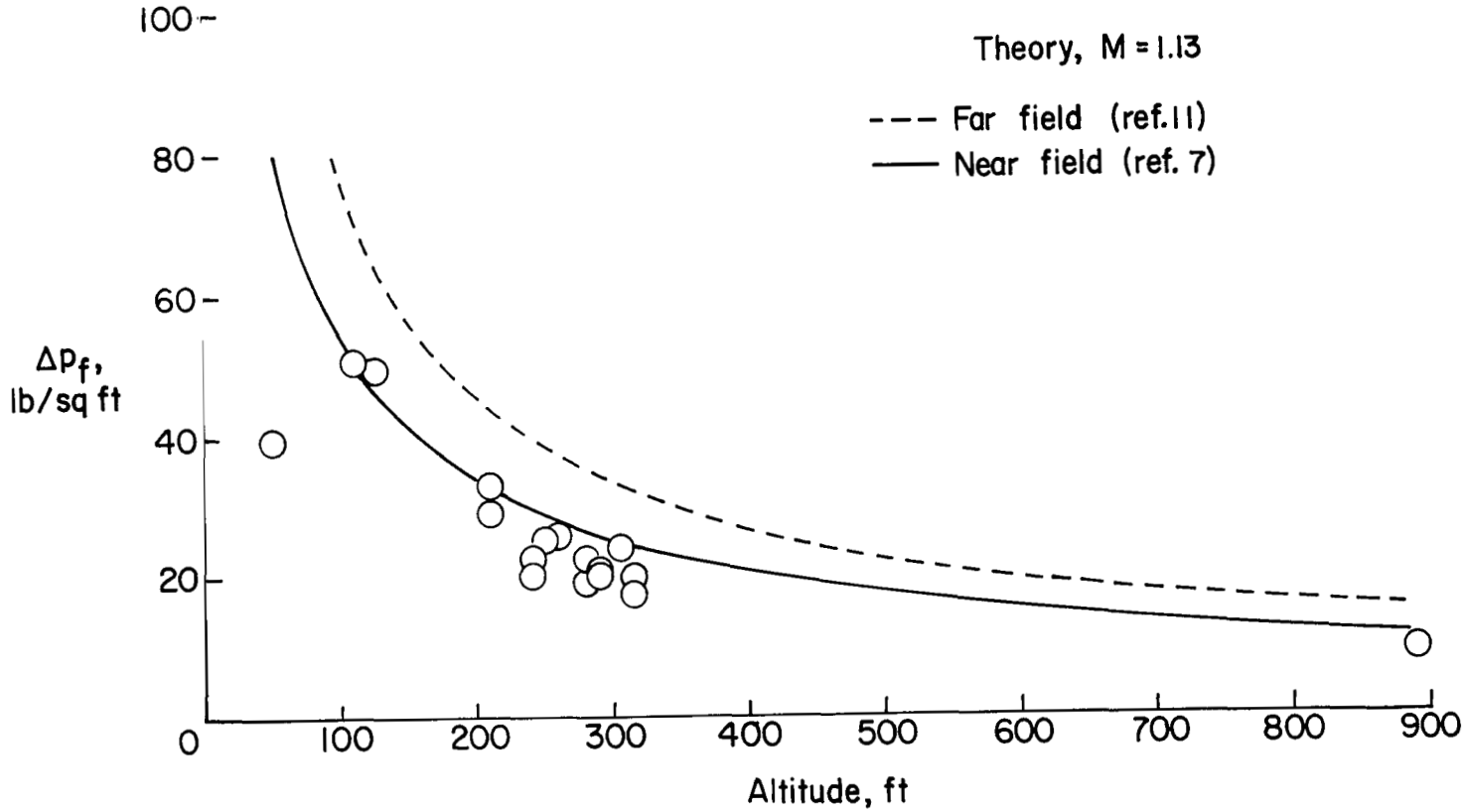

(b) Pressures measured in free air.

Figure 21.- Concluded.

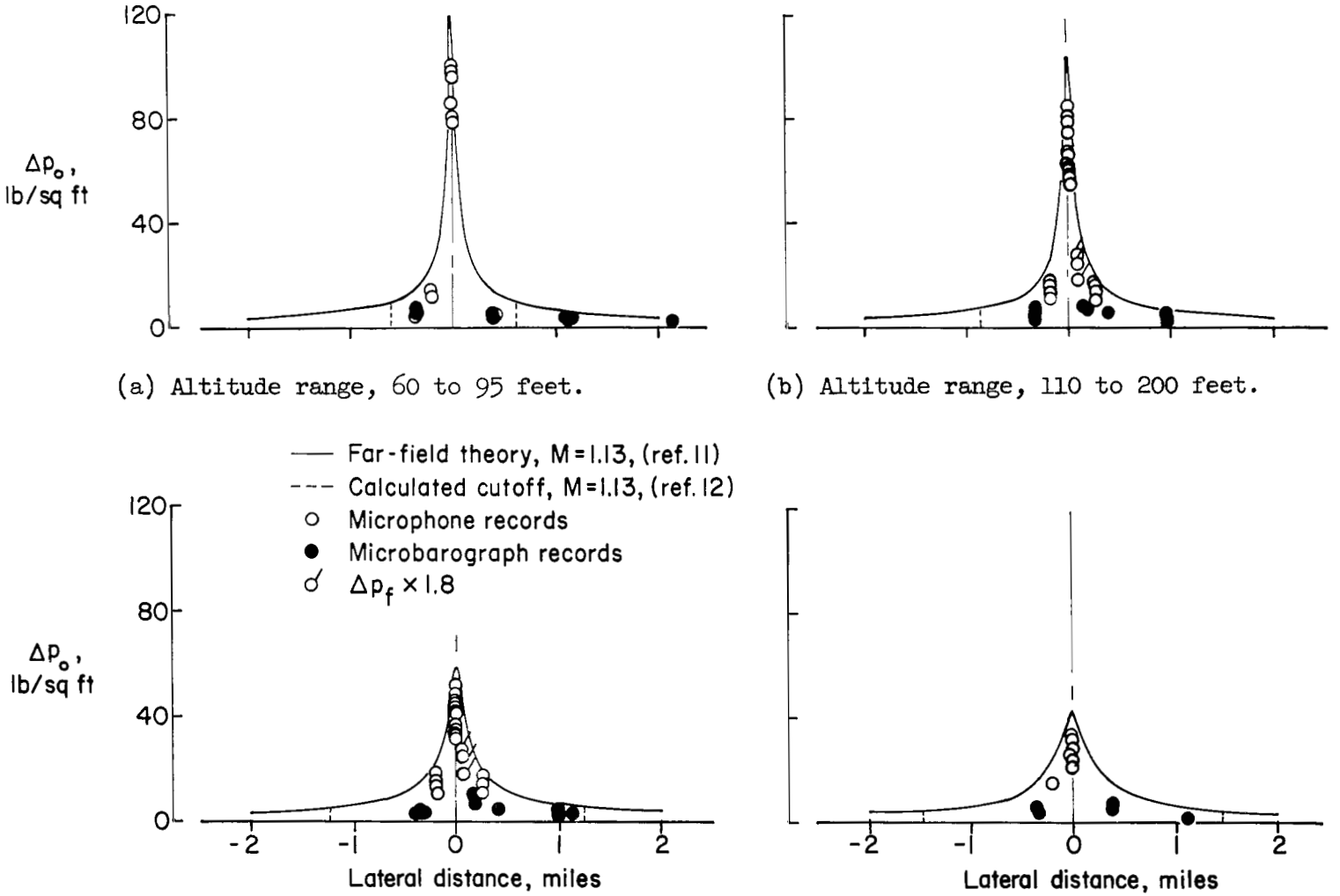

(a) Altitude range, 60 to 95 feet.

(b) Altitude range, 110 to 200 feet.

(c) Altitude range, 270 to 380 feet.

(d) Altitude range, 485 to 590 feet.

Figure 22.- Ground measurements of shock-wave pressures as function of lateral distance from flight path for airplane A.

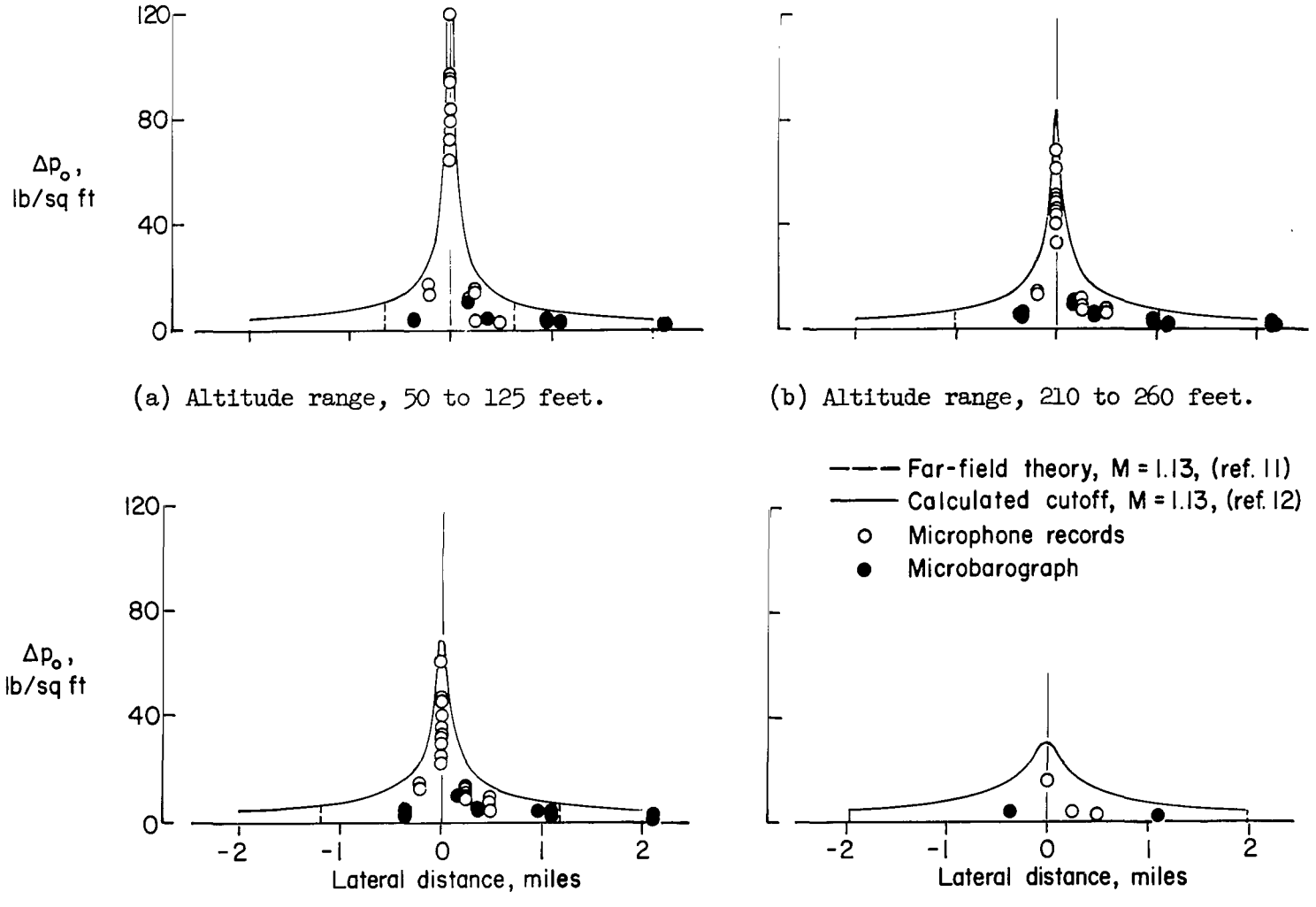

(a) Altitude range, 50 to 125 feet.

(b) Altitude range, 210 to 260 feet.

(c) Altitude range, 280 to 320 feet.

(d) Altitude, 890 feet.

Figure 23.- Ground measurements of shock-wave pressures as function of lateral distance from flight path for airplane B.

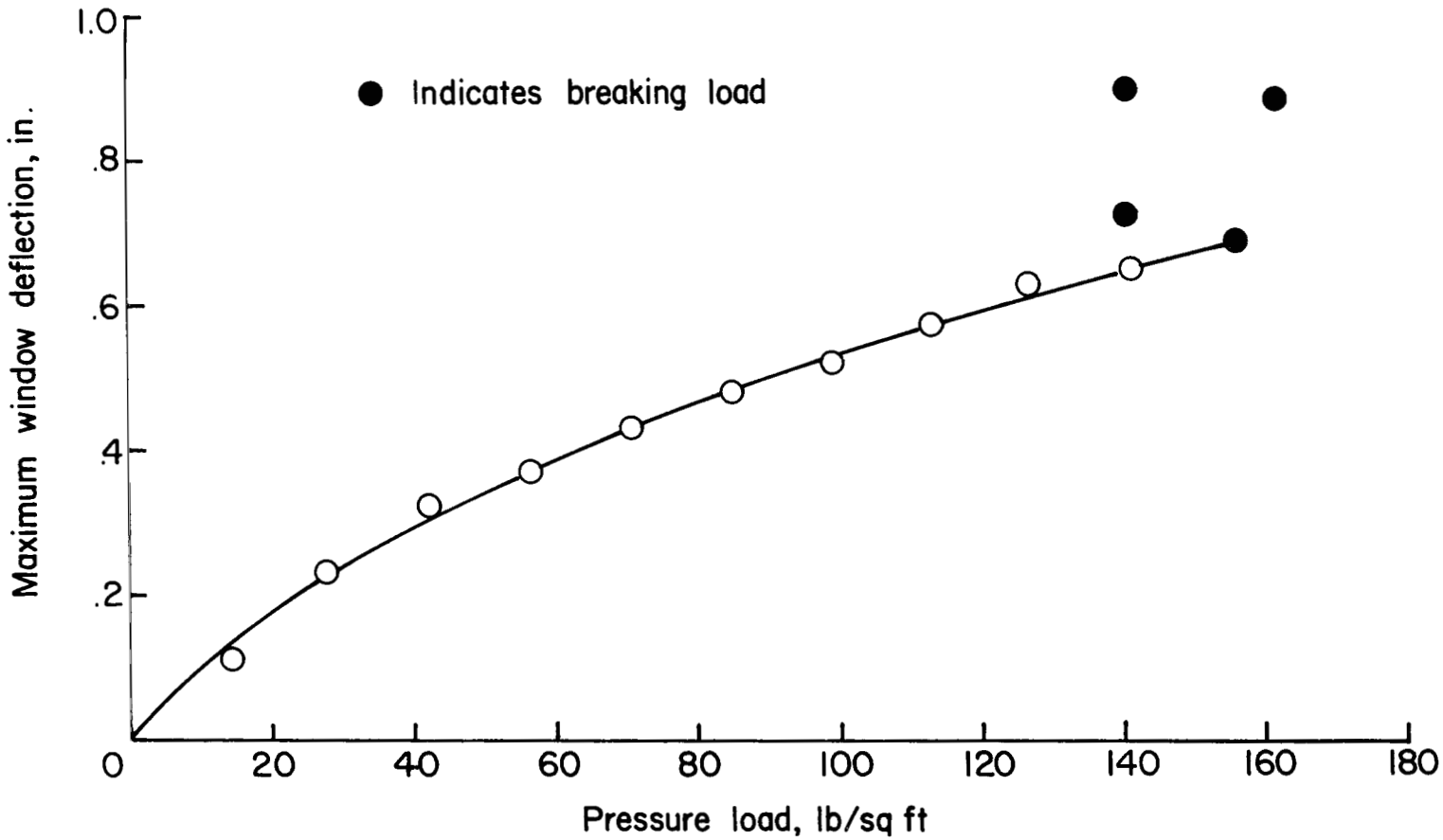

Figure 24.- Results of static breaking tests of 3- by 3-foot plain windows having double-strength glass.

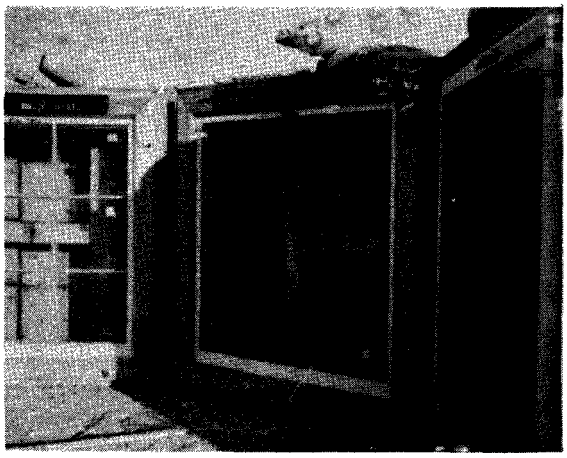

(a) Plain and colonial windows in bay arrangement.

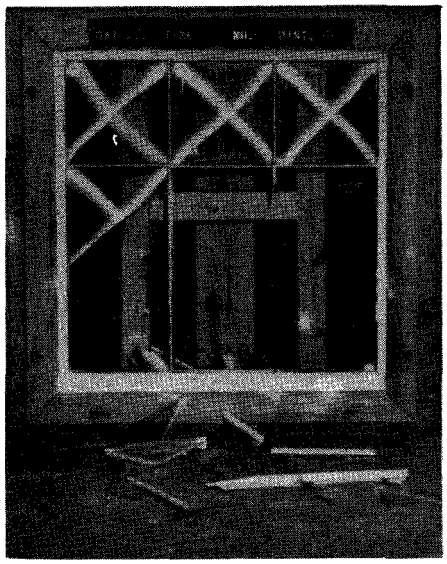

(b) Colonial window in single cubicle.

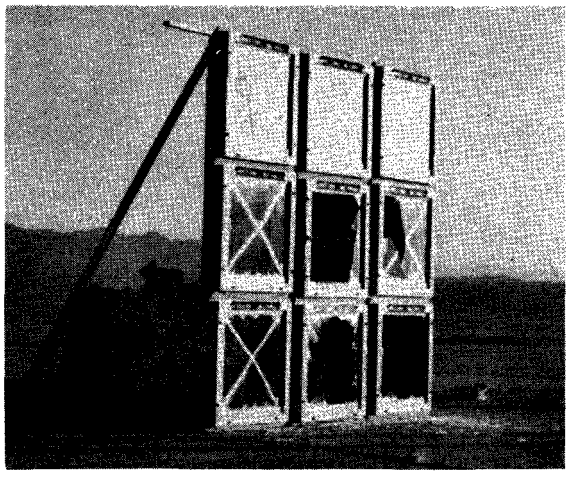

(c) Plain windows in stacked arrangement.

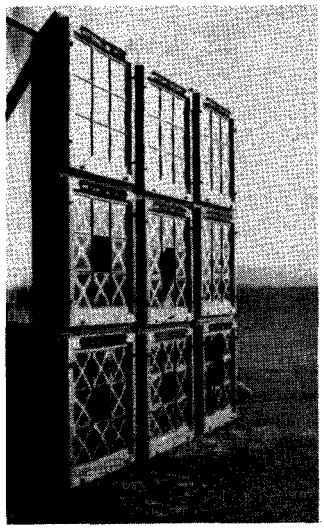

(d) Colonial windows in stacked arrangement.

L-61-5103

Figure 25.- Photographs of window damage.

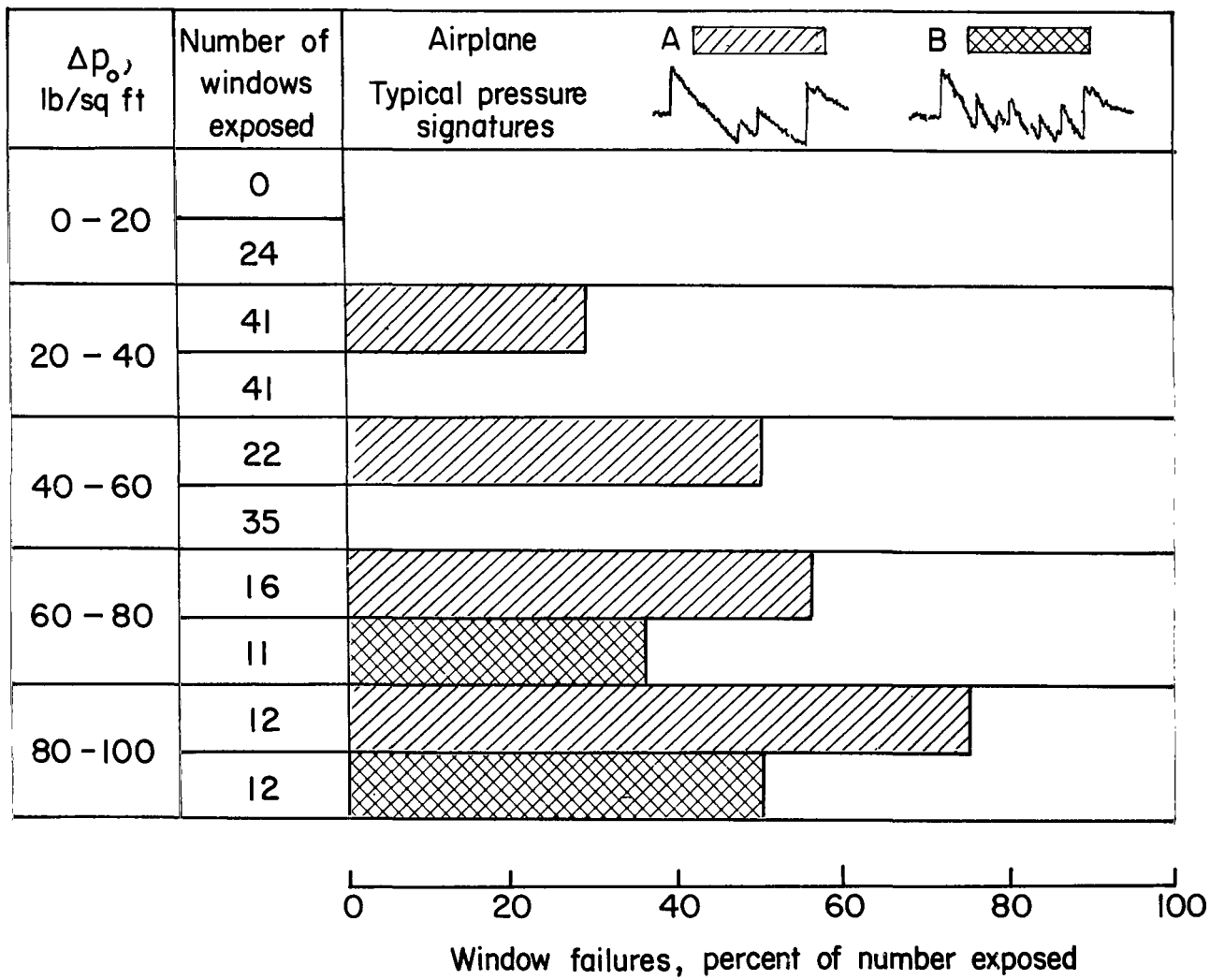

Figure 26.- Bar graph summary of the results of shock-wave induced window-glass breakage associated with flight tests at very low altitudes of two fighter airplanes.

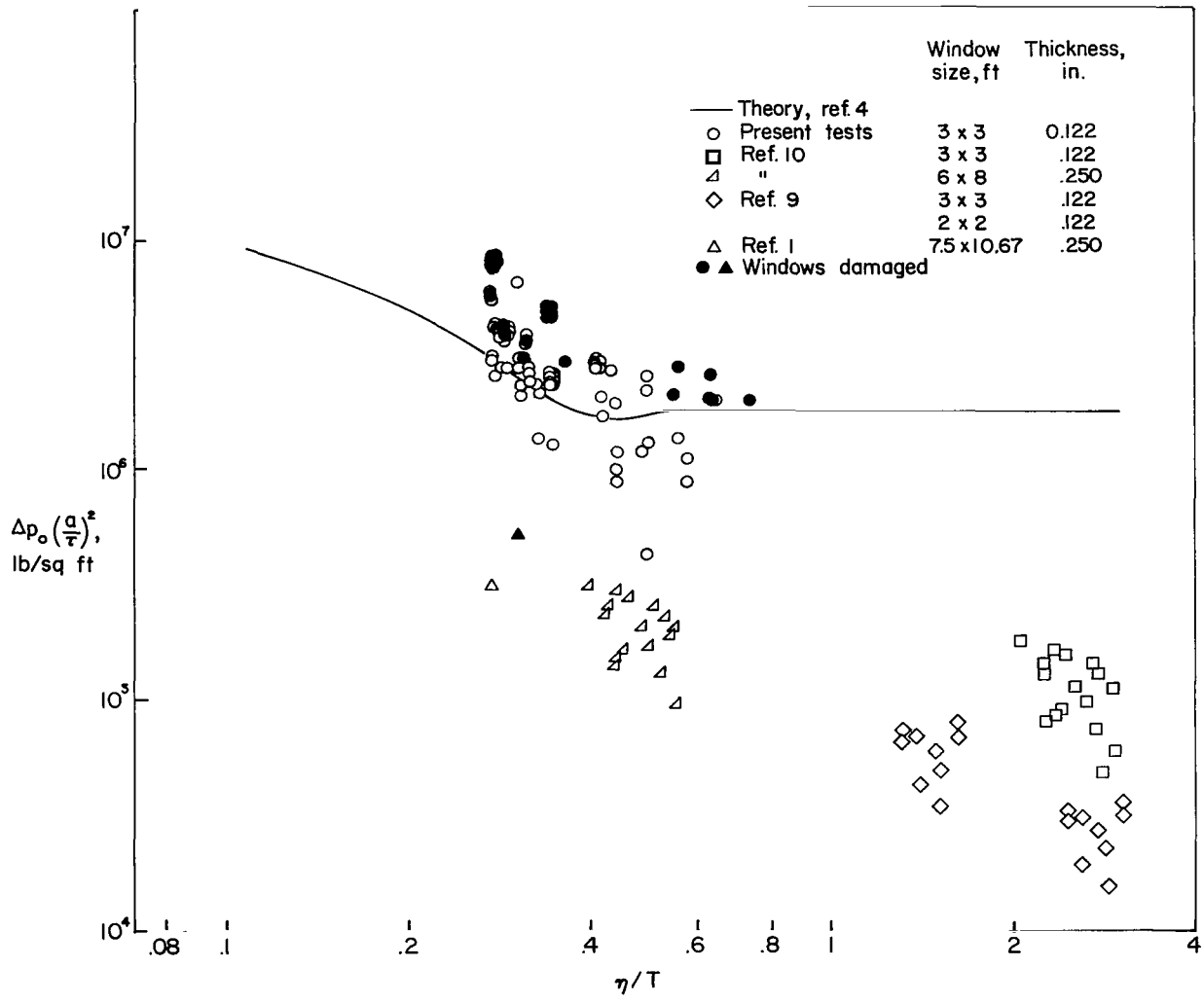

Figure 27.- Summary of window-glass breakage experience due to sonic booms.

"The aeronautical and space activities of the United States shall be conducted so as to contribute . . . to the expansion of human knowledge of phenomena in the atmosphere and space. The Administration shall provide for the widest practicable and appropriate dissemination of information concerning its activities and the results thereof."

—NATIONAL AERONAUTICS AND SPACE ACT OF 1958

NASA SCIENTIFIC AND TECHNICAL PUBLICATIONS

TECHNICAL REPORTS: Scientific and technical information considered important, complete, and a lasting contribution to existing knowledge.

TECHNICAL NOTES: Information less broad in scope but nevertheless of importance as a contribution to existing knowledge.

TECHNICAL MEMORANDUMS: Information receiving limited distribution because of preliminary data, security classification, or other reasons.

CONTRACTOR REPORTS: Technical information generated in connection with a NASA contract or grant and released under NASA auspices.

TECHNICAL TRANSLATIONS: Information published in a foreign language considered to merit NASA distribution in English.

TECHNICAL REPRINTS: Information derived from NASA activities and initially published in the form of journal articles.

SPECIAL PUBLICATIONS: Information derived from or of value to NASA activities but not necessarily reporting the results of individual NASA-programmed scientific efforts. Publications include conference proceedings, monographs, data compilations, handbooks, sourcebooks, and special bibliographies.

Details on the availability of these publications may be obtained from:

SCIENTIFIC AND TECHNICAL INFORMATION DIVISION

NATIONAL AERONAUTICS AND SPACE ADMINISTRATION

Washington, D.C. 20546